Integrated stratigraphy of the Lower and Middle Cenomanian in a Tethyan section (Blieux, southeast France) and correlations with Boreal basins

Stéphane Reboulet [a,*], Fabienne Giraud [b], Claude Colombié [a], André Carpentier [a]

[a] UMR 5276, CNRS, Laboratoire de Géologie de Lyon, Terre Planètes Environnement, Université Lyon 1-ENS Lyon, Bâtiment Géode, 2 rue Raphaël Dubois, 69622 Villeurbanne cedex, France
[b] ISTerre, UMR 5275, Université de Grenoble 1, 1381 rue de la piscine, BP 53, 38041 Grenoble cedex 9, France

ABSTRACT

A detailed stratigraphic analysis was carried out on the Lower–Middle Cenomanian hemipelagic deposits of the Blieux section (Alpes-de-Haute-Provence; southeast France) in order to identify the Middle Cenomanian event I (MCE I) in the Vocontian Basin. These deposits are represented by five bundles composed of limestone–marl alternations that are separated by thick marly intervals. The Blieux section, which is well exposed, very thick, continuous and relatively rich in macrofauna, provides an ideal succession for an integrated approach. Biostratigraphy by ammonoids and sequence stratigraphy have been established for the whole succession whereas calcareous nannofossil and geochemical analyses have been carried out on a restricted interval across the Lower/Middle Cenomanian boundary. The uppermost part of the *Mantelliceras mantelli* Zone, the *Mantelliceras dixoni* Zone and the lower part of the *Acanthoceras rhotomagense* Zone have been recognized. The appearance of the genus *Cunningtoniceras* (*C. inerme* or *C. cunningtoni*) is used to place the base of the *A. rhotomagense* Zone and the Lower/Middle Cenomanian boundary. This boundary is also well characterized by the presence of nannofossil Subzone UC2C. Two orders of hierarchically stacked depositional sequences have been identified. Medium- and large-scale sequences correspond to 400 ky eccentricity cycles and to third-order cycles, respectively. The duration of the interval studied (from the uppermost part of the *M. mantelli* to the lower part of the *A. rhotomagense* zones) is estimated to be 2.8 my. Carbon-isotope values determined from bulk carbonate sediments show a first positive excursion (+0.6‰) corresponding to the MCE Ia, in the lower part of the *A. rhotomagense* Zone. A subsequent increase (+1.1‰) is recorded and could correspond to MCE Ib, but a sharp return to baseline values as expected in an excursion is not observed. The duration of the MCE I is estimated to be less than 400 ky. The Blieux section is correlated with some classical sections of the Anglo-Paris (Southerham, Folkestone, Cap Blanc-Nez) and Lower Saxony (Baddeckenstedt and Wunstorf) basins using ammonoid biostratigraphy, sequence stratigraphy, and chemostratigraphy. It is proposed as a candidate for the Middle Cenomanian GSSP (Global Boundary Stratotype Section and Point).

© 2012 Elsevier Ltd. All rights reserved.

1. Introduction

The "mid-Cenomanian event" was first described by Paul et al. (1994). This event, present in both Boreal and Tethyan domains, is characterized by two small positive carbon ($\delta^{13}C$) isotope excursions (Paul et al., 1994; Gale, 1995; Mitchell et al., 1996; Jarvis et al., 2001, 2006). The first peak (+0.5‰ at Folkestone, England, used as the standard section) corresponding to the "Middle Cenomanian event" (MCE Ia; Mitchell et al., 1996) begins in the *Cunningtoniceras inerme* Zone (Jarvis et al., 2001, 2006), and is associated with

a lowstand systems tract (Gale, 1995). The second peak (+0.8‰ in the Folkestone section) corresponds to MCE Ib (Mitchell et al., 1996) and is located in the lowermost part of the *Acanthoceras rhotomagense* Zone (Jarvis et al., 2001, 2006). It is associated with a transgressive systems tract (Gale, 1995; Mitchell et al., 1996).

For the Lower and the Middle Cenomanian in northwestern Europe, detailed lithological, biostratigraphic and isotopic data are available only from successions of chalks, marly chalks and limestones of the Anglo-Paris, Cleveland and Lower Saxony basins (Juignet and Kennedy, 1976; Gale, 1990, 1995; Amédro et al., 1994, 1997; Paul et al., 1994; Mitchell et al., 1996; Mitchell and Carr, 1998; Robaszynski et al., 1998; Wilmsen and Niebuhr, 2002; Wilmsen, 2003). For the Tethyan area, one section in the deep western Basque Basin in Spain has been investigated for biostratigraphy based

on planktonic foraminifera and carbon isotope (Rodriguez-Lazaro et al., 1998). Other pelagic sections in Central Italy (Jenkyns et al., 1994; Erbacher et al., 1996; Erbacher and Thurow, 1997; Stoll and Schrag, 2000) and the Betic Cordillera (Stoll and Schrag, 2000), and a hemipelagic section of the Briançonnais domain (Strasser et al., 2001) have been studied for this time interval. However, these sections are very condensed with uniform lithologies: the entire Cenomanian is less than 60 m thick in the three sections of Bottacione, Contessa Quarry (where limestones with chert nodules are dominant) and Santa Ines; and the entire Cenomanian is around 15 m thick in the Briançonnais domain. Furthermore, the biostratigraphic and carbon isotopic records are not precise enough to allow good correlations with northwestern Europe. The Cenomanian of the Kalaat Senan region (Central Tunisia) has been described and compared with the Cenomanian of western Europe (Robaszynski et al., 1993, 1994), but detailed correlations and a detailed carbon-isotope record are not available. The Cenomanian–Turonian of the Moroccan sections at Azazoul Road and Mohammed Beach (Tarfaya Basin) have been studied for micropalaeontology, biostratigraphy and carbon isotopes, but the Middle Cenomanian is represented by only few metres of sediments in these shallow-marine settings (subtidal and middle shelf palaeoenvironments; Kuhnt et al., 2009; Gertsch et al., 2010). The Upper Cretaceous hemipelagic sediments of the Vocontian Basin (southeastern France) have been examined for the Albian/Cenomanian (Gale et al., 1996; Kennedy et al., 2000) and Cenomanian/ Turonian (Crumière, 1989; Grosheny and Malartre, 1997; Grosheny et al., 2006; Takashima et al., 2009; Fernando et al., 2010) boundaries, but only a few studies were focused on the Cenomanian itself (Crumière, 1989; Gale, 1995) and none of these includes stable isotope geochemistry and calcareous nannofossils; moreover, the ammonoid biostratigraphy is not precise.

The aim of this work is to (1) determine whether MCE I is present in southeastern France (Giraud et al., 2008); (2) establish a detailed biostratigraphic framework with both ammonoids and calcareous nannofossils; and (3) propose detailed correlations between the subtropical basin of the northern Tethys margin (Vocontian Basin) and mid-latitude northwest European shelf-sea basins, using, bio, chemo and sequence stratigraphy. The Blieux section in the Alpes-de-Haute-Provence, Vocontian Basin, provides an ideal succession for an integrated approach owing to the expanded, continuous and well-exposed outcrops and relatively abundant fossil records (in particular ammonoids).

2. Geological setting

In the Early Cretaceous, the tectonic regime in the Vocontian Basin was extensional with strike-slip movements. Beginning with the Late Albian, compression or transpression dominated (Rubino, 1989; Kandel, 1992). The resulting rhomboidal Vocontian Basin is regarded as a pull-apart basin marking the transition between the Bay of Biscay/Pyrenean rift in the southwest and the Valaisan domain in the northeast (Ferry and Rubino, 1989). During the Albian, an uplift of all the basin margins occurred and was responsible for the emergence of the Durance Isthmus, south of the Provence Platform (Masse and Philip, 1976). Consequently, a strong differential subsidence occurred between the Provence carbonate shelf to the south, with carbonate and siliciclastic facies, and the Vocontian Basin to the north, with limestone–marl alternations, representing hemipelagic to subpelagic sediments (Conard, 1983). On the Provence carbonate shelf at the southern margin of the Durance Isthmus, two rudist-bearing formations are identified; the first of these is dated as Late Albian–Early Cenomanian, the second as Mid Cenomanian–Late Cenomanian (Philip, 1978). From the Mid Cenomanian to Santonian, the Durance Isthmus represented

a stable, emergent landmass of low relief between the Pyreneo-Provençal Sea and the Alpine Sea that was invaded by marine transgressions (Rubino, 1989).

The Blieux section is located on the southern margin of the Vocontian Basin and is in a key position to record palaeoenvironmental changes between proximal areas (platform environments) and the pelagic realm (Fig. 1). As already described by Cotillon (1971), Blieux is one of the few sections where ammonoids are relatively abundant. Benthic macrofauna is also well represented and bivalves are locally abundant (Bréhéret, 1997). This section has previously been studied for the Oceanic Anoxic Event 1d (Breistroffer interval; Giraud et al., 2003; Reboulet et al., 2005).

3. Material and methods

3.1. Sedimentology

Sedimentological analysis and sequence stratigraphy are used to interpret the dynamics of the sedimentary systems. First, a detailed bed-by-bed logging, including thickness and lithology, allows the definition of medium- and large-scale depositional sequences, which are hierarchically stacked (Strasser et al., 1999). Medium-scale sequences are smaller than large-scale sequences, but they display almost the same sedimentary features. Then, these field observations together with palaeogeographical and stratigraphical data available in Philip (1978) and Crumière (1991) as well as our new palaeontological and geochemical results allow a sequence-stratigraphical framework to be proposed. The sequence-stratigraphical interpretation is based on the concepts of Mitchum et al. (1977), Haq et al. (1987), and Posamentier et al. (1988). However, the classical geometries of systems tracts cannot be distinguished in metre-scale
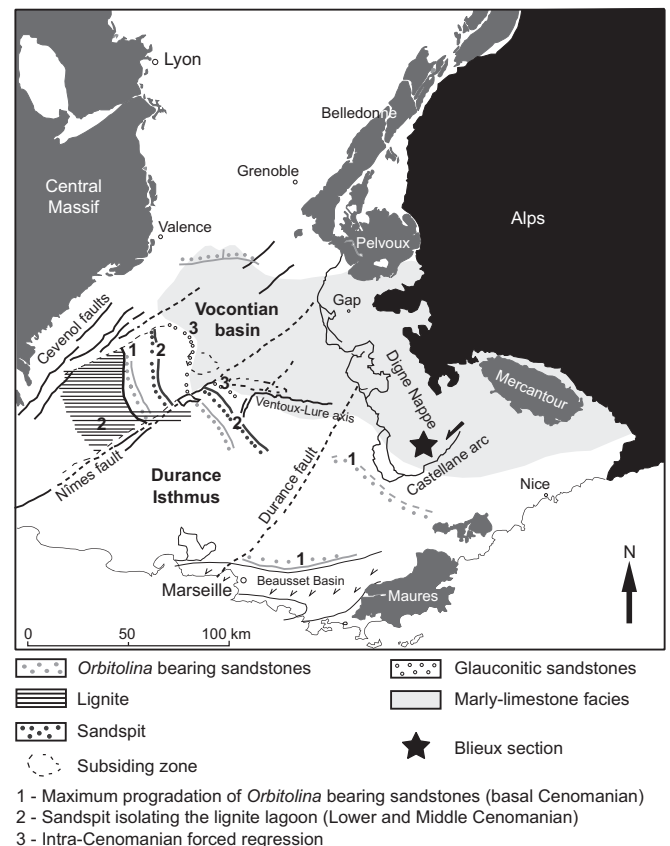

Fig. 1. Palaeogeographic map of southeastern France during the Early and Mid-Cenomanian, redrawn from Briais (2010), with location of the Blieux section.

sequences (Strasser et al., 1999). Consequently, deposits are used instead of systems tracts. The boundaries between these deposits correspond to sequence stratigraphic surfaces such as sequence boundaries (SBs), transgressive surfaces (TSs), and maximum-flooding zones (MFZs; Fig. 2). Changes in lithology in lowstand deposits (LSDs) and highstand deposits (HSDs) reflect depositional environments that are more and more proximal (i.e., close to land). SBs develop between HSDs and LSDs. Transgressive deposits (TDs) form between TSs and MFZs. TSs correspond to rapid changes in lithology that reflect changes from the relatively most proximal to the relatively most distal environments (Strasser et al., 1999). MFZ is used instead of maximum-flooding surface (MFS) when MFSs are not developed (Strasser et al., 1999). Transgressive parts of the observed sequences correspond to TDs and end by MFZs. Regressive parts include HSDs and LSDs and form between MFZs and TSs. TSs coincide with the end of regressions (i.e., the change from progradation to retrogradation according to Catuneanu et al., 2009).

Stratigraphical correlation with previously studied successions of the same age in the Anglo-Paris and Lower Saxony basins lends further support to the proposed sequence-stratigraphical interpretation. The duration of ammonoid zones combined with the number of depositional sequences defined in this work allows a cyclostratigraphical interpretation that provides additional information of factors that controlled sedimentation in the Vocontian Basin during the Cenomanian and helped to place the MCE I and to infer its duration.

3.2. Geochemistry

Isotope geochemistry and calcimetry have been carried out in a 92-m-thick interval, from layers 494 to 649 (Fig. 2) within which the MCE I is expected.

Forty-five samples corresponding to different lithologies were analysed for carbon and oxygen isotopes. Stable isotope measurements were obtained from bulk sediment using an automated mass spectrometer (VG Isocarb plus Optima) combined with a common-acid bath. The isotopic data were obtained using standard methods of gas-source mass spectrometry following acid dissolution with 100% phosphoric acid. Isotope values are reported as per mil relative to Vienna Pee Dee Belemnite. The analytical precision is <0.1‰ for both $\delta^{13}C$ and $\delta^{18}O$ measurements.

Forty-seven samples were analysed for calcium carbonate content. It was determined using the carbonate bomb technique, which measures CO_2 pressure during a hydrochloric acid attack.

3.3. Ammonoids

The sampling of macrofaunal assemblages was carried out at 96 levels, from layers 300 to 648 (Fig. 2). The marly intervals were not sampled because the outcrop conditions are less favourable. The selected interval of the Blieux section was studied for its content of pelagic macrofauna (715 ammonoids or around 81% of the macrofauna; 3 belemnites) and benthic macrofauna (140 inoceramids and 28 sea urchins; around 16% and 3% of the macrofauna, respectively). Aptychi and rhyncholites are absent, as in the uppermost Albian of the same section (Reboulet et al., 2005).

The identification of ammonoids at species level is often difficult or impossible because of the relatively poor preservation of the material in the Blieux section; specimens doubtfully identified are indicated by a question mark on some figures. Dissolution of shells is the norm and specimens are preserved as internal calcareous moulds. Their fragmentation is relatively frequent and compaction is important, particularly for the phragmocones. Consequently, some characteristics, such the whorl section and the strength of

ribs and tubercules, and how they change between the inner and outer whorls, cannot be observed and compared.

The material is stored in the palaeontological collections of the Department of Geology at the Claude Bernard University of Lyon, France (collection of Reboulet). Ammonoids figured here were coated with ammonium chloride before they were photographed.

3.4. Calcareous nannofossils

Among the samples selected for calcimetry (from layers 494 to 632; Fig. 2), 41 were prepared using the random settling technique of Geisen et al. (1999), a method adapted from Beaufort (1991). This allows the calculation of absolute abundances. Different longitudinal transverse sections were observed under a light polarizing microscope at a magnification of ×1560 in order to find biostratigraphic markers. The taxonomic frameworks of Perch-Nielsen (1985) and Burnett et al. (1998) are followed. The nannofossil biostratigraphic zones applied to the section investigated are the UC zones of Burnett et al. (1998) and Lees (2002). The nannofossil preservation was evaluated following the classes defined by Roth (1983).

4. Results

4.1. Sedimentology

4.1.1. Description of the Blieux section

The section studied contains three different parts (Fig. 2). The lower part (from layers 280 to 310) is mainly composed of alternating thick marly interbeds and thin silty or sandy limestone beds; these alternations locally include silty levels, which are interpreted as turbidites (Crumière, 1991). The middle part (from layers 310 to 560) is more calcareous; it principally contains marl–limestone alternations with some silty turbidites and slumps. The upper part (from layers 560 to 648) is more argillaceous; it is composed of marl–limestone alternations that locally contain slumps. The middle part includes four calcareous bundles, which correspond to thick intervals that are more calcareous than the rest of the section (bundle 1, layers 310–422g; bundle 2, layers 440–476; bundle 3, layers 494–516; bundle 4, layers from 522 to 560). They contain thin marly interbeds and numerous thick calcareous beds. Given these criteria, two additional calcareous bundles can be defined: one in the lower part of the section (from layers 290 to 292) and one in the upper part (bundle 5, from layers 590 to 648). Crumière (1991) also identified similar calcareous bundles in another Cenomanian section (Vergons) of the Vocontian Basin.

4.1.2. Sedimentary features of depositional sequences, hierarchy and stacking pattern

In the Blieux section studied, stratigraphic surfaces are not developed. Consequently, the definition of medium- and large-scale sequences mainly depends on changes in lithology and thickness of calcareous beds and marly interbeds (Fig. 2). Medium-scale sequences are the easiest to define. Apart from bundle 5, which ends the section, calcareous bundles are followed by a thick marly interval intersected by a thin calcareous interval, which is formed by a group of more calcareous alternations (Fig. 2). These successions characterize medium-scale sequences. The section contains seven complete medium-scale sequences (41 m thick on average) that stack into large-scale sequences. Bundles 1 and 4 are different from bundles 2, 3 and 5 and constitute the lower part of large-scale sequences (Fig. 2): bundle 1 is very thick (48 m as opposed to around 12 m for the others); bundle 4 appears to be more calcareous than the others because the marly interbeds are generally thinner than in the other bundles; the upper part of
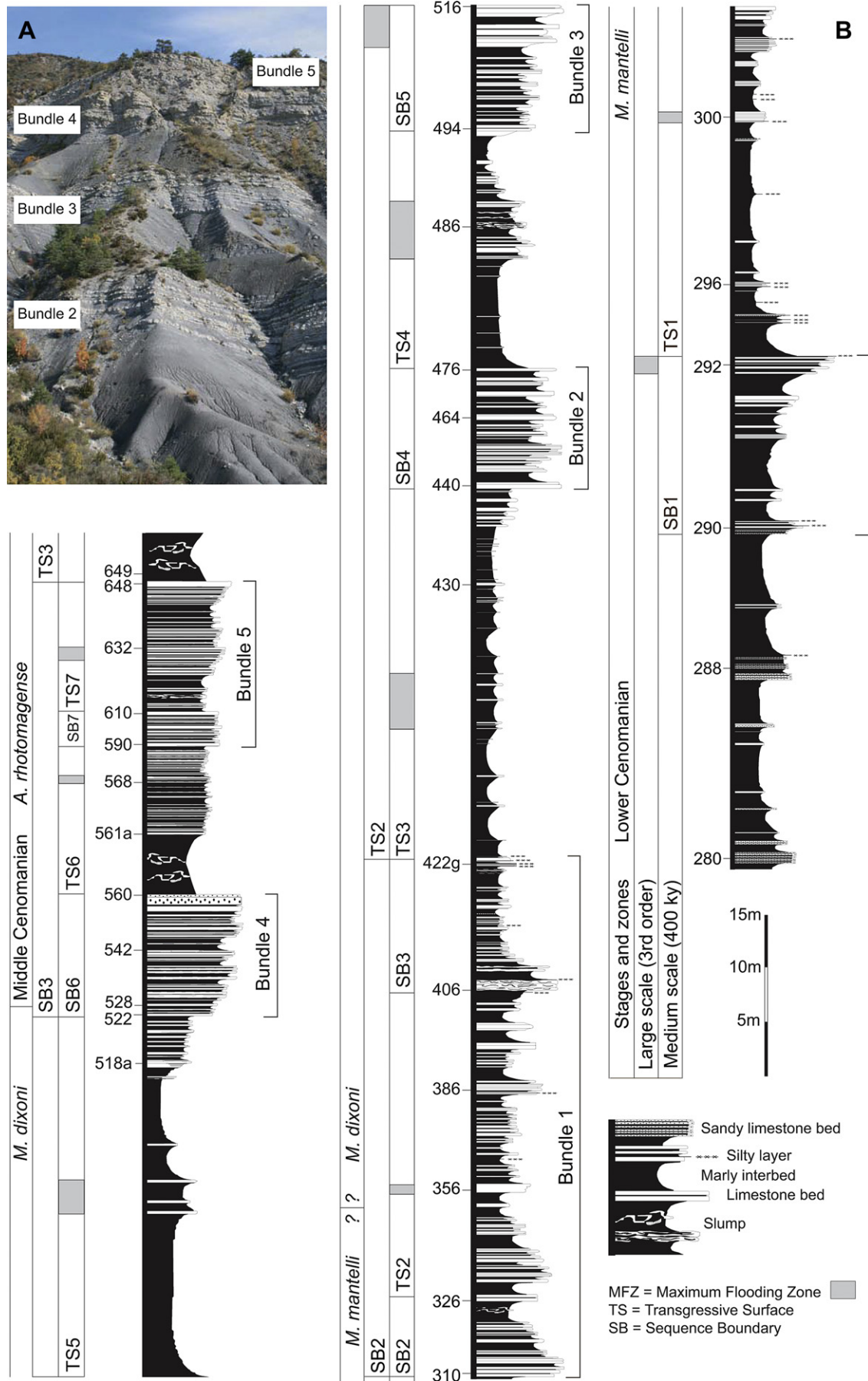
Fig. 2. A, photograph of the Blieux section (from bundles 2 to 5). B, lithological column and depositional sequences for the Lower and Middle Cenomanian of the Blieux section.

bundles 1 and 4 contains sandy limestone beds (several layers for bundle 1 and beds 558 and 560 for bundle 4) in contrast to calcareous bundles 2, 3 and 5, which only include limestone beds. The first large-scale sequence is incomplete. The second large-scale sequence mainly corresponds to the *Mantelliceras dixoni* Zone. It is 157 m thick and contains four medium-scale sequences. The base of the third large-scale sequence approximately coincides with the boundary between the *M. dixoni* and *A. rhotomagense* zones.

4.2. Ammonoids

4.2.1. Systematics

The Cenomanian ammonoid fauna of the Blieux section consists of 15 genera grouped into 11 families and seven super-families, using the classification proposed by Wright et al. (1996) and emended by Klein et al. (2009) for Phylloceratoidea (Appendix; Fig. 3). The palaeontological study of the ammonoids by Carpentier (2007) was reviewed and completed for the present paper. As this is not the place to propose a systematic revision, only a few comments on some taxa are included here. Further information is available in the papers of Boule et al. (1906), Wright and Wright (1949), Collignon (1964), Renz (1968), Kennedy and Hancock (1970), Kennedy (1971), Thomel (1972, 1992), Scholz (1973, 1979), Juignet and Kennedy (1976), Kennedy and Cobban (1976), Marcinowski (1980), Kennedy et al. (1981, 1986), Kennedy and Juignet (1983, 1984, 1993), Wright and Kennedy (1984, 1987, 1995, 1996), Cooper (1994, 1998, 1999), Gale et al. (1996), Wright et al. (1996), Kaplan et al. (1998), Lehmann (1998), Joly (2000), Monnet (2005) and Wilmsen and Mosavinia (2011).

Acanthoceras (*A. rhotomagense*; Fig. 4A) and *Cunningtoniceras* (*C. cunningtoni*, Fig. 4B; *C. inerme*, Fig. 4C) are rare; only nine specimens of each genus have been found (Fig. 3). Kennedy (1971), Wright and Kennedy (1987) and Kennedy and Juignet (1993) underlined the fact that there are transitional forms between *C. inerme* and *C. cunningtoni*. The specimen of *Cunningtoniceras* from layer 536b of the Blieux section (Fig. 4C) and identified as *C. inerme* could be transitional to *C. cunningtoni*. *Mantelliceras* is more abundant, but the identification of different species is difficult because it is partly based on the whorl section and tuberculation and their modification during ontogeny (see descriptions of Wright and Kennedy, 1984 and Kennedy et al., 1986). Specimens of *Mantelliceras* found in the Blieux section are generally incomplete and flattened; consequently, only a few specimens have been doubtfully identified as *M. mantelli* (Fig. 4D), *M. dixoni* (Fig. 4E) and *M. picteti*. *Schloenbachia* is dominant in many layers of the Blieux section (Fig. 3) but only *S. varians* (Fig. 4F) is considered here; a high phenotypic plasticity of *S. varians* from northeast Iran has been observed by Wilmsen and Mosavinia (2011), who suggested that *S. coupei* could be placed in the synonymy with it. *Hyphoplites* (*H. campichei*, *H. costosus* (Fig. 5A), *H. curvatus* and *H. falcatus*), *Puzosia* (*P.* (*P.*) *mayoriana*; Fig. 5B), *Hyporbulites* (probably *H. seresitensis*) and *Tetragonites* are rare to very rare in the Blieux section (Fig. 3). Among heteromorphs, Turrilitidae are represented by six species belonging to three genera (Fig. 3): *Hypoturrilites mantelli*, *H. tuberculatus*, *Mesoturrilites aumalensis*, *M. corrugatus*, *Turrilites scheuchzerianus* (Fig. 5C) and *T. costatus* (Fig. 5D). *Sciponoceras* is relatively abundant and limited to the uppermost part of the section (Fig. 3). All specimens probably belong to *S. baculoides* (Fig. 5E). Other genera of Turrilitoidea are represented by a few specimens that are relatively poorly preserved and their identification is doubtful; *Anisoceras* and *Hamites* are represented by *A. plicatile* (Fig. 5F) and probably by *H. simplex*, respectively (Fig. 3). Among *Scaphites*, only *S. obliquus* (Fig. 5G) has been identified in the section.

4.2.2. Biostratigraphic implications

A revised zonation of the Cenomanian for southeastern France and Western Europe was proposed by Monnet and Bucher (1999, 2002). This is a sequence of discrete unitary association zones called UA-zones. It comprises ammonoid data from epicontinental basins of Western Europe located on the Northern Tethyan margin. It is in good agreement with the empirical zonation (assemblage zones) developed for the Anglo-Paris Basin by Wright and Kennedy (1984). Consequently, the standard zonation (Wright and Kennedy, 1984), revised by Monnet and Bucher (1999, 2002, 2007; see also Monnet et al., 2003), is used for the Blieux section.

As pointed out by Thomel (1992), the Lower Cenomanian of the Blieux section is difficult to characterize. The appearance of *M. dixoni*, which traditionally defines the base of its assemblage zone (Kennedy, 1969; Kennedy and Hancock, 1971), is recorded in layer 354 (Fig. 3).

The lowermost part of the Blieux section probably corresponds to the *Mantelliceras mantelli* Zone, because the index-species has been found in the lower part of bundle 1 (Fig. 3). However, *M. mantelli* is not restricted to its zone, where this species is common, but can occur as a rarity also in the *M. dixoni* Zone (Kennedy, 1971; Juignet and Kennedy, 1976; Wright and Kennedy, 1984). The age of the *M. mantelli* Zone seems to be confirmed by the presence of *Hypoturrilites mantelli* and *H. tuberculatus* (turrili-cones) that have been found just below bundle 1 (layers 300 and 302, respectively; Fig. 3). *H. mantelli* is scarce and seems restricted to the lower part of the Lower Cenomanian (Kennedy and Juignet, 1983; *M. mantelli* Zone in England according to Kennedy, 1971 and Wright and Kennedy, 1996). *H. tuberculatus* occurs in the Lower Cenomanian and is especially common in the *M. mantelli* Zone (Kennedy and Juignet, 1983; Wright and Kennedy, 1996). According to Monnet and Bucher (2002, 2007), *H. mantelli* and *H. tuberculatus* are restricted to the *M. mantelli* Zone.

In the Blieux section, *Mantelliceras* is relatively frequent in bundles 1 and 2, less abundant in bundle 3 and absent in bundle 4 (Fig. 3). Some specimens have been doubtfully identified as *M. dixoni*. This index-species is restricted to its zone (Wright and Kennedy, 1984). In the upper part of its range, *Mantelliceras* co-occurs with *Mesoturrilites aumalensis* (Fig. 3); this has been recognized in the *M. dixoni* Zone of Eastbourne, Sussex (Wright and Kennedy, 1996). In the Blieux section, *S. obliquus* occurs from layers 420e–f to 484 (Fig. 3). This species appears in the upper part of the Lower Cenomanian in Sarthe, France ("Sables et grès de Lamnay", *M. dixoni* Zone) and in southern England (Juignet and Kennedy, 1976). According to Wright and Kennedy (1996), *S. obliquus* appears in the *M. mantelli* Zone (in its uppermost part according to Monnet and Bucher, 2002), but it is fairly common in the *M. dixoni* Zone. The co-occurrence of *M. dixoni*, *M. aumalensis* and *S. obliquus* would indicate the presence of the *M. dixoni* Zone in the Blieux section, so the range of *Mantelliceras* is similar to that observed in the Anglo-Paris Basin. *Turrilites scheuchzerianus* characterizes the upper Lower and lower Middle Cenomanian (Lehmann, 1998; Monnet and Bucher, 2002) and seems to be common in the *M. dixoni* Zone and the lower part of the *A. rhotomagense* Zone (Wright and Kennedy, 1996). In the Blieux section, it is rare and recorded only around the boundary between these two zones (Fig. 3).

Following the recommendations of the 1976 Cenomanian Symposium in Paris, the base of the Middle Cenomanian is defined by the first appearance of the genera *Acanthoceras* and *Cunningtoniceras* above beds with *Mantelliceras* (Kennedy's unpublished 1995 report in Tröger and Kennedy, 1996; Ogg et al., 2004). At the 1995 Brussels symposium, it was emphasized by Tröger and Kennedy (1996) that the lowest Mid-Cenomanian faunas in the Northern Temperate Realm and Tethyan Realm are characterized by different species of *Cunningtoniceras* (*C. inerme* and *C. cunningtoni*)
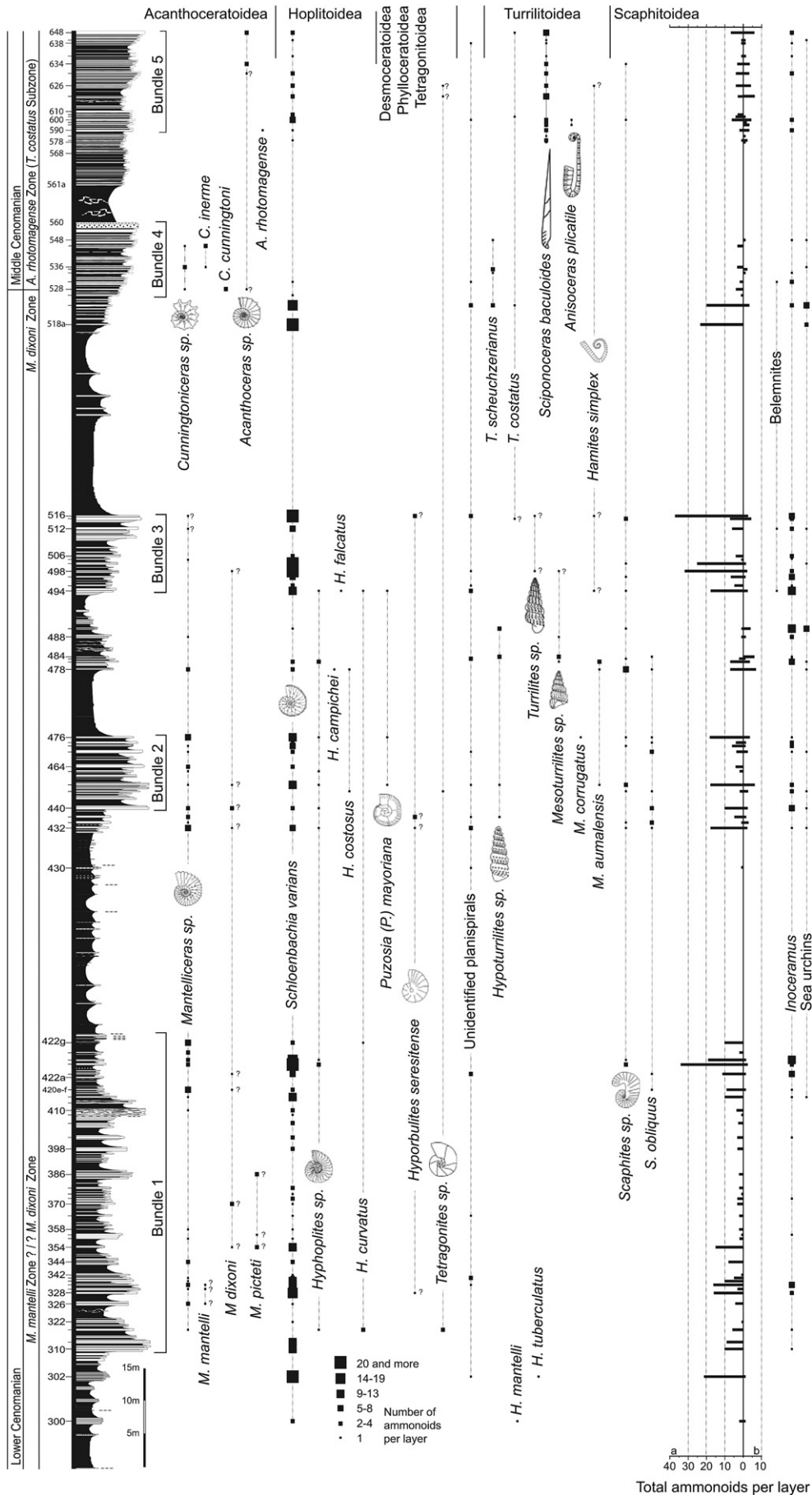
Fig. 3. Stratigraphic distribution of ammonoids and the zonal scheme for the Blieux section. Specimens doubtfully identified are indicated by a question mark.
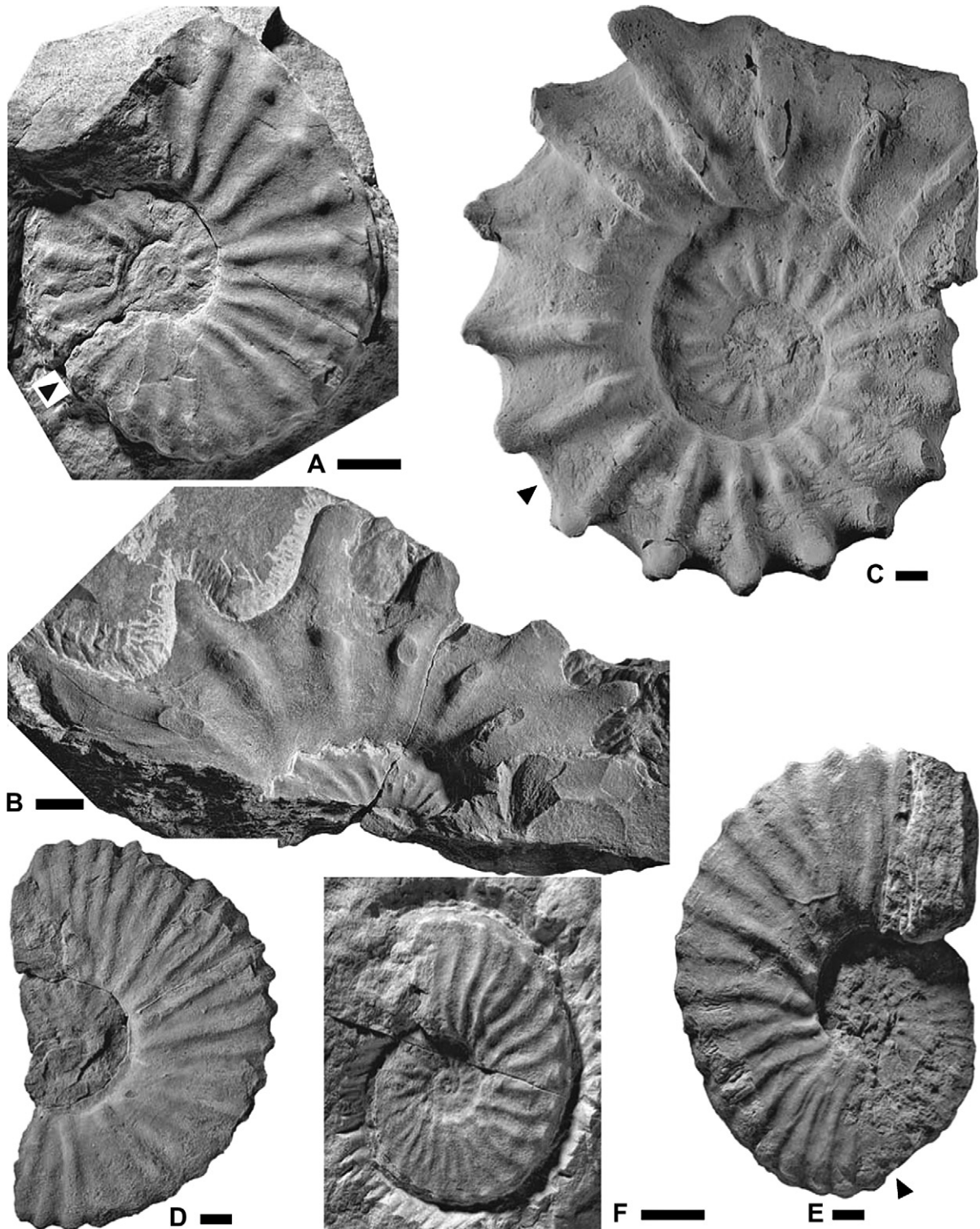
Fig. 4. Ammonoids of the Blieux section (collection of Reboulet, FSL, Faculté des Sciences de Lyon, Department of Geology, University of Lyon, France). A, *Acanthoceras rhotomagense* (Brongniart), FSL 338301, BLX 590, *A. rhotomagense* Zone. B, *Cunningtoniceras cunningtoni* (Sharpe), FSL 338302, BLX 528, *A. rhotomagense* Zone. C, *Cunningtoniceras inerme* (Pervinquière), FSL 338303, BLX 536b, *A. rhotomagense* Zone. D, *Mantelliceras mantelli* (?) (Sowerby), FSL 338304, BLX 332, *M. mantelli* Zone. E, *Mantelliceras dixoni* (?) Spath, FSL 338305, BLX 354, *M. dixoni* Zone. F, *Schloenbachia varians* (Sowerby), FSL 338306, BLX 418, *M. dixoni* Zone. Scale bars represent 1 cm; black arrows indicate end of phragmocone.

rather than *A. rhotomagense*. These authors recommended that the base of the Middle Cenomanian substage be defined by the first appearance of *C. inerme*; however, they did not mention the *C. inerme* Zone proposed by Gale (1995) for the Western European zonation, which is defined by the earlier appearance of *C. inerne*

with respect to *Acanthoceras*; this interval zone was previously introduced in the zonation of Central Tunisia as the first zone of the Middle Cenomanian (Robaszynski et al., 1993, 1994; Gale, 1995). In order to follow the standard zonation of Wright and Kennedy (1984) based on the association principle, the *A. rhotomagense*
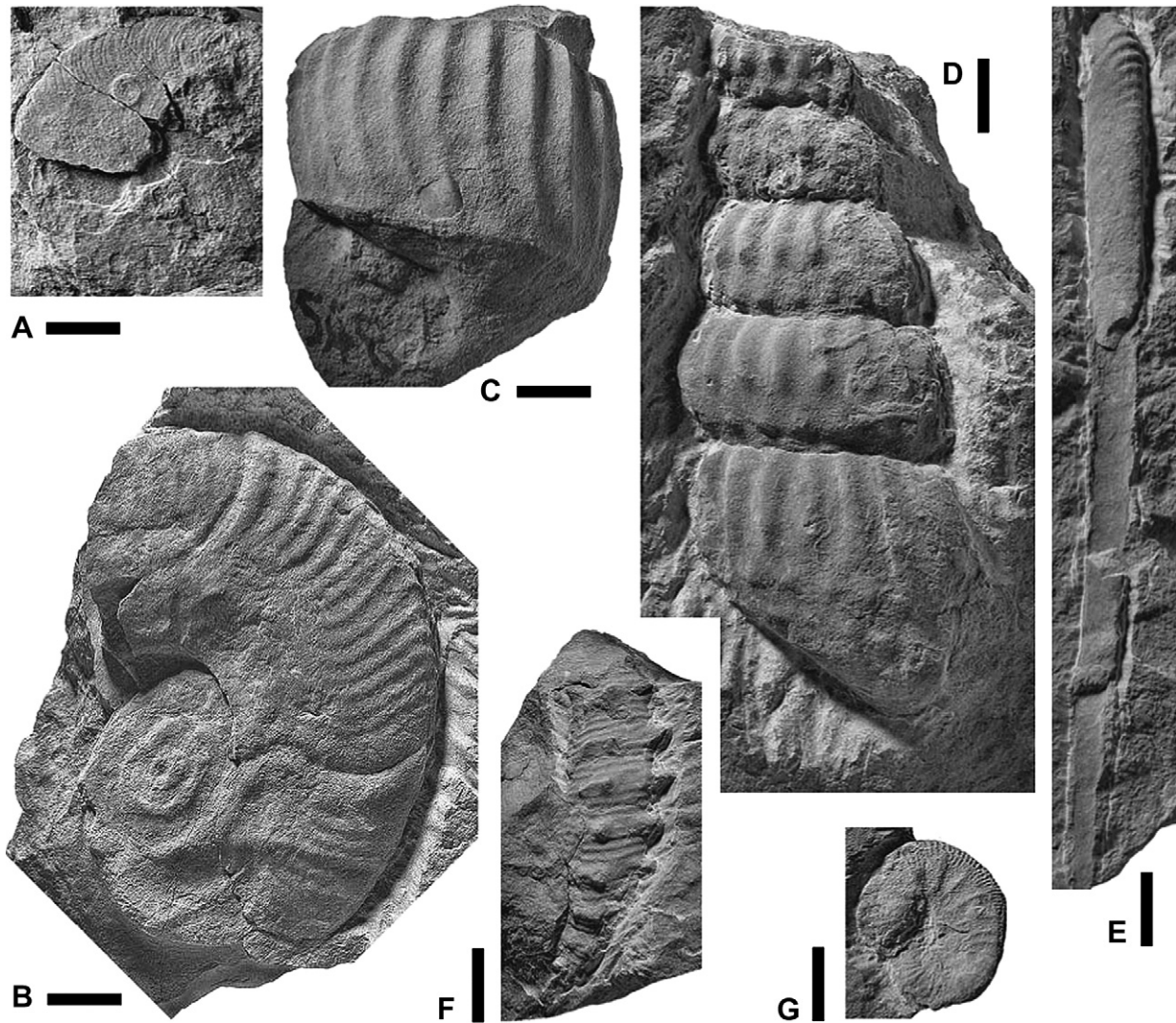
Fig. 5. Ammonoids of the Blieux section (collection of Reboulet, FSL, Faculté des Sciences de Lyon, Department of Geology, University of Lyon, France). A, *Hyphoplites costosus* Wright and Wright, FSL 338307, BLX 446-448, *M. dixoni* Zone. B, *Puzosia* (*Puzosia*) *mayoriana* (d'Orbigny), FSL 338308, BLX 454, *M. dixoni* Zone. C, *Turrilites scheuchzerianus* Bosc, FSL 338309, BLX 548, *A. rhotomagense* Zone. D, *Turrilites costatus* Lamarck, FSL 338310, BLX 604, *A. rhotomagense* Zone. E, *Sciponoceras baculoides* (Mantell), FSL 338311, BLX 634, *A. rhotomagense* Zone. F, *Anisoceras plicatile* (Sowerby), FSL 338312, BLX 596, *A. rhotomagense* Zone. G, *Scaphites obliquus* Sowerby, FSL 338313, BLX 440, *M. dixoni* Zone. Scale bars represent 1 cm.

Zone could be kept as the first zone of the Middle Cenomanian. Indeed, *C. inerme* and *A. rhotomagense* are part of the diagnostic association of the first UA-zone (n° 15) of the Middle Cenomanian of the Vocontian, Anglo-Paris and Münster basins (see Figs. 5 and 7 in Monnet and Bucher, 2002). UA-zone 15 of the northwest Europe is correlated with UA-zone 10 of Central Tunisia, which is included in the *C. inerme* interval Zone (Fig. 7 in Monnet and Bucher, 2007). *C. inerme* is a synchronous taxon (sensu Monnet and Bucher, 2007; UA-zone 5 = *A. rhotomagense* Zone) and it is a good species on which to place, by its appearance, the base of the *A. rhotomagense* Zone in northwest Europe and the base of the Middle Cenomanian in Europe, North Africa (Central Tunisia) and the USA (Western Interior). As *C. cunningtoni* also characterizes the UA-zone 5 in northwest Europe and the Western Interior (Monnet and Bucher, 2007), this species could also be used when *C. inerme* is absent. Consequently, the base of the *A. rhotomagense* Zone, and the base of the Middle Cenomanian, could be defined by the presence of *Cunningtoniceras.* In the Blieux section, the appearance of this genus (*C. inerme* or *C. cunningtoni*) is used to place the base of the *A. rhotomagense* Zone and so the base of the Middle Cenomanian. The position of the Lower/Middle Cenomanian boundary

(first *C. cunningtoni* in layer 528; Fig. 3) is confirmed by the absence of *Mantelliceras*, *Hyphoplites* and *Mesoturrilites* in bundles 4 and 5, as these genera are unknown in the Middle Cenomanian (Kennedy and Juignet, 1984; Wright and Kennedy, 1984, 1996; Monnet and Bucher, 2002, 2007).

The *Turrilites costatus* and *T. acutus* subzones of the *A. rhotomagense* Zone, defined in the Anglo-Paris Basin (Wright and Kennedy, 1984), have no correlatives in the UA-zones of the Münster and Vocontian basins; this subdivision is not justified in terms of associations (Monnet and Bucher, 2002, 2007). However, Kennedy (1969) underlined the fact that the upper part of the *T. costatus* assemblage is well characterized by the great abundance of *S. baculoides* whereas this species is rare in the *T. acutus* assemblage. This faunal change (greater abundance in heteromorphs) in the upper part of the *T. costatus* Subzone of the *A. rhotomagense* Zone was also observed in other parts of the Anglo-Paris Basin (Kennedy and Hancock, 1970; Kennedy and Juignet, 1975, 1983; Juignet and Kennedy, 1976; Juignet, 1977; Wright and Kennedy, 1995), in the Münster and Lower Saxony basins (Owen, 1996; Kaplan et al., 1998; Wilmsen, 2003) and in southwestern Crimea (Marcinowski, 1980).

In the Vocontian Basin, the lower part of the *A. rhotomagense* Zone (*T. costatus* Subzone) is also well characterized by the presence of *S. baculoides* (Vergons section; Thomel, 1991) and by its abundance (Saint-Lions section; Thomel, 1992). In the Blieux section, the *T. costatus* Subzone is well characterized by the presence of the index-species (Fig. 3; for its occurrence in the uppermost Lower Cenomanian, see Lehmann, 1998, p. 38), and by the appearance of *S. baculoides* in the lowermost part of the Middle Cenomanian (layer 578) and its abundance in bundle 5 (Fig. 3). In conclusion, the greater abundance of *S. baculoides* in the *A. rhotomagense* Zone is recognized over a large palaeogeographic area and its acme constitutes a good biostratigraphic marker in the upper part of the *T. costatus* Subzone.

4.3. Calcareous nannofossils

4.3.1. Assemblages

All nannofossil taxa observed by Carpentier (2007) in the Blieux section are reported in a distribution chart given in the Table S1 (online supplementary data). In general, the preservation of nannofossils is fair, with moderately etched and overgrown specimens (categories E2 and O2). Some assemblages are well preserved with only slightly etched and overgrown nannofossils (categories E1 and O1). Some are also poorly preserved with strongly etched and moderately or strongly overgrown specimens (categories E3 and O2, and E3 and O3 only for one sample). Eight coccolith taxa represent more than 85% of the total assemblage of nannofossils, which is composed of 89 species; the dominant taxa are, in decreasing abundance: *Watznaueria barnesiae*, *Biscutum ellipticum*, *Prediscosphaera* spp., *Tranolithus orionatus*, small *Zeugrhabdotus*, *Rhagodiscus achlyostaurion*, *Eiffelithus turriseiffelii* and *Cretarhabdus* spp. The most abundant species and biostratigraphic markers are illustrated in Fig. 6.

4.3.2. Nannofossil biostratigraphy

The nannofossil biozonation scheme of Burnett et al. (1998) is used. Based on the stratigraphic distribution of the marker taxa (Fig. 7, Table S1), the interval studied can be assigned to nannofossil zones UC2–UC3 (Lower to Middle Cenomanian). The resulting nannofossil biostratigraphy correlates very well with the ammonoid biostratigraphy established in this study (Fig. 7).

UC2 Zone of Burnett et al. (1998; Lower Cenomanian).

The presence of *Gartnerago segmentatum* in the lowest samples selected for quantitative analyses allows the base of this interval to be assigned to Zone UC2. This zone is subdivided into three subzones (UC2a, UC2b and UC2c). The base of Subzone UC2b is defined by the last occurrence (LO) of *Lordia xenota* and the base of Subzone UC2c by the first occurrence (FO) of *Cylindratus sculptus*. In the Blieux section, the LO of *L. xenota* occurs at the same level as the FO of *C. sculptus* (sample 517d; Table S1). In this case, this suggests that Subzone UC2b cannot be recognized in the Blieux section. However, *L. xenota* has been identified in only two levels (samples 497 and 517d) and is very rare (Table S1). This could indicate that bundle 3 can be dated to the UC2b Subzone. Taking into account these two hypotheses, the denomination UC2a–b is used in the nannofossil zonal scheme (Fig. 7).

UC3 Zone of Burnett et al. (1998; Middle Cenomanian).

The FO of *Lithraphidites acutus* is recognized in sample 537 (Table S1). The occurrence of *Gartnerago theta* in the highest samples of the section suggests that only Subzone UC3a defined by Burnett et al. (1998) is present in the Blieux section (Fig. 7).

4.4. Geochemistry

The stable carbon-isotope data vary between +0.7 and +2‰ (Fig. 7). In the lower part of the succession, from bundle 3 to the middle part of the overlying marly interval, a general decrease of 0.6‰ is recognized, followed by an increase of the same order of amplitude to the interval just below bundle 4. Carbon-isotope values increase from 0.9‰ at the base of bundle 4 (= base of the *A. rhotomagense* Zone) to 1.5‰ in its upper part (layers 544 and 548); this forms a marked positive excursion. After a sharp and short decrease just before the end of bundle 4, carbon-isotope values begin a long-term rise within the *A. rhotomagense* Zone with a plateau at around 2‰ starting below bundle 5. A weak decrease is observed across bundle 5.

The stable oxygen-isotope record varies between −4.8 and −2.7‰ (Fig. 7). The lower part of the succession, from bundle 3 to the base of bundle 4, shows lower mean values than the rest of the succession. At the top of bundle 4, the oxygen-isotope values are characterized by rapid fluctuations with a high amplitude (2.1‰; from layers 522a to 558). Towards the top of the succession, a slight increase is recognized, interrupted by a short-term decrease.

The calcium carbonate content varies from 24.7 to 72.6% (Fig. 7), showing that alternations are composed of argillaceaous marls or marls in the interbeds and marly limestones in the beds.

5. Interpretation

5.1. Geochemical record of the Blieux section

The marked positive excursion of δ^{13}C in the lower part of the *A. rhotomagense* Zone could represent Middle Cenomanian Event Ia. A second positive trend is recorded after this, where maximum values (2‰) could correspond to MCE Ib; the return to baseline values as would be expected for a true excursion is not observed (Fig. 7). Also in sections from the Lower Saxony Basin, there is not really a return to background values above MCE Ib (Wilmsen and Niebuhr, 2002). Nevertheless, this positive shift of around 1‰ (from 0.9‰ in the upper part of bundle 4 to maximum values of 2‰) is more important than the MCE Ib excursions recognized in other sections in the Anglo-Paris Basin (Paul et al., 1994; Jarvis et al., 2006). The plateau observed above MCE Ib could be owing to a high sedimentation rate, which could also explain the formation of large slumps (see 5.2.).

The carbon-isotope values recorded in the Blieux section are lower than those recorded in hemipelagic and pelagic carbonate sediments deposited in other basins during the Early–Mid-Cenomanian time interval: the bulk carbon-isotope values recorded in hemipelagic chalk successions in northwest Europe are between 1.3 and 2.9‰ (Speeton, South Ferriby and Rheine sections, Mitchell et al., 1996; Escalles section, Paul et al., 1994; Southerham

Fig. 6. Light microscope photographs of selected nannofossil species from the Blieux section. A, *Axopodorhabdus albianus*, XLP, sample 517d. B, *Biscutum ellipticum*, XLP, sample 517d. C, *Broinsonia signata*, XLP, sample 517d. D, *Corollithion kennedyi*, XLP, sample 517d. E, F, *Cylindratus sculptus*. E, TL, sample 539. F, XLP, sample 539. G, *Eiffelithus turriseiffelii*, XLP, sample 517d. H, *Gartnerago nanum*, XLP, sample 517d. I, *Gartnerago theta*, XLP, sample 517a. J, K, *Lithraphidites acutus*. J, TL, sample 551. K, XLP, sample 551. L, M, *Lithraphidites pseudoquadratus*. L, TL, sample 517d. M, XLP, sample 517d. N, *Lordia xenota*, XLP, sample 517d. O, *Placozygus* cf *P. fibuliformis*, XLP, sample 520. P, *Prediscosphaera columnata*, XLP, sample 517d. Q, *Retecapsa crenulata*, XLP, sample 517d. R, *Rhagodiscus achlyostaurion*, XLP, sample 517d. S, *Tranolithus orionatus*, XLP, sample 517d. T, *Watznaueria barnesiae*, XLP, sample 503. U, *Zeugrhabdotus bicrescenticus*, XLP, sample 503. V, *Zeugrhabdotus diplogrammus*, XLP, sample 503. W, *Zeugrhabdotus* cf *Z. embergeri*, XLP, sample 517d. X, *Zeugrhabdotus noeliae*, XLP, sample 517d. XLP, cross polarized light; TL, transmitted light. Scale bar represents 2 μm.
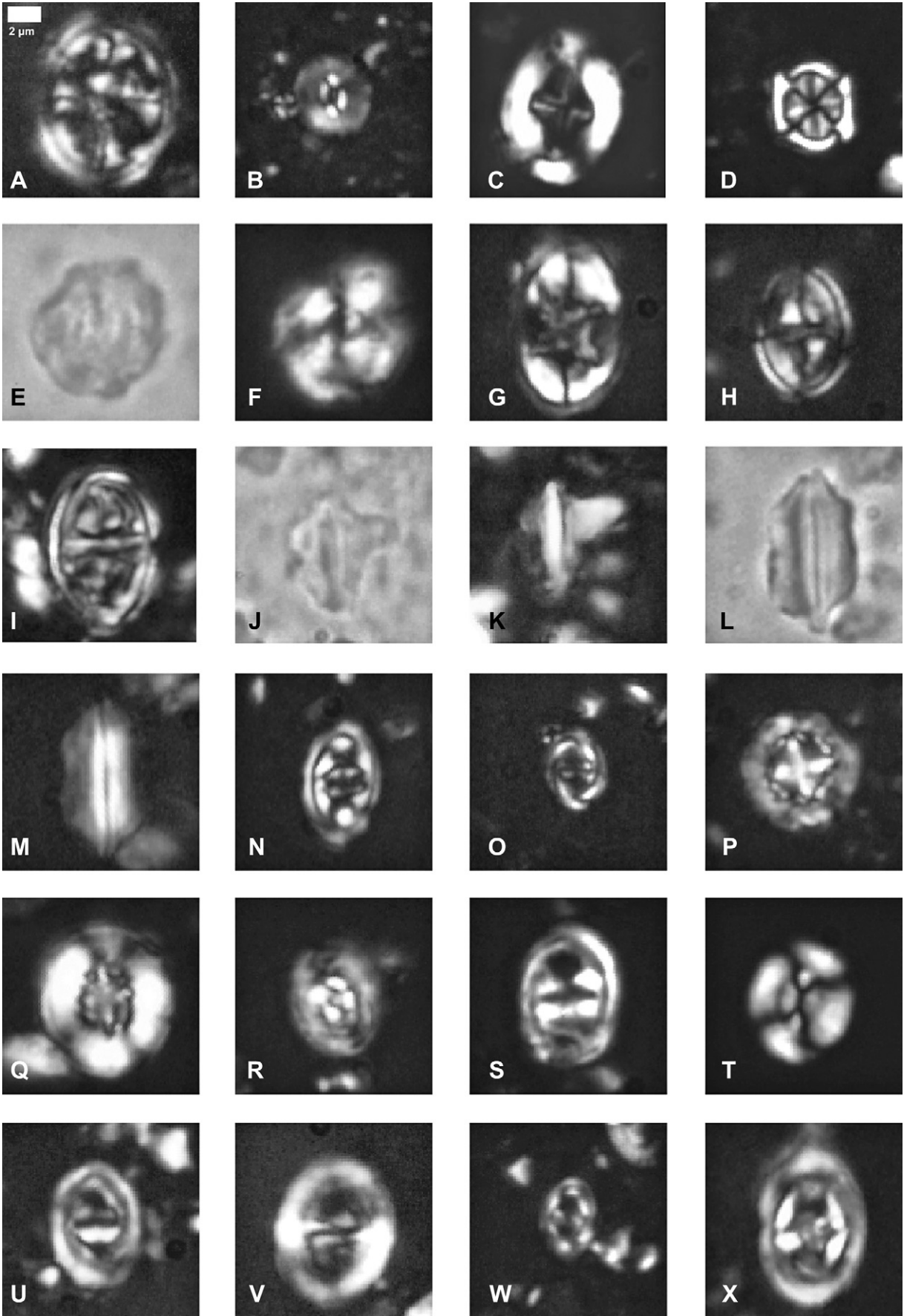
section, Paul et al., 1994; Wilmsen, 2007; Folkestone section, Paul et al., 1994; Mitchell et al., 1996; Culver Cliff section, Paul et al., 1994; Jarvis et al., 2001; Dover section, Jarvis et al., 2006; Wunstorf section, Mitchell et al., 1996; Wilmsen, 2007; Baddeckenstedt and Hoppenstedt sections, Wilmsen, 2007). In the coeval pelagic Tethyan successions of Central Italy, carbon-isotope values vary between 0.8 and 3.1‰ (Piobicco area, Erbacher et al., 1996; Erbacher and Thurow, 1997; Bottacione Gorge section, Jenkyns et al., 1994; Contessa Quarry section, Stoll and Schrag, 2000).

The carbonate phase in all analysed Blieux samples consists of calcite of different origins. The biogenic pelagic carbonate fraction is composed of nannofossils and planktonic foraminifera. The negative correlation found between $CaCO_3$ and the nannofossil absolute abundance shows that nannofossils contribute only a minor part of the carbonate fraction, especially in samples with $CaCO_3$ higher than 60% (Fig. 8A). The biogenic fraction also contains macrofauna represented by ammonoids and bivalves (Pectinoidea). Previous studies on the uppermost Albian of the Blieux section have demonstrated that the autochthonous carbonate fraction (nannofossils, ammonoids and bivalves) is negatively correlated with the calcium carbonate content (Giraud et al., 2003; Reboulet et al., 2005). Allochthonous carbonate imported from the platform is not negligible for the Albian (Giraud et al., 2003). During the Mid Cenomanian, the Provence Platform was characterized by rudist carbonate facies (Philip, 1978). A contribution of platform-derived carbonate mud to the Cenomanian hemipelagic micrites of the Blieux section would lead to lighter $\delta^{13}C$ values, since proximal marine settings present lighter $\delta^{13}C$ values with respect to slope and basinal settings (Immenhauser et al., 2008). Platform-derived carbonate in the sediments of the Blieux section can therefore explain the lower $\delta^{13}C$ values measured there when compared to other Tethyan sections.

Carbon and oxygen-isotope values in limestones can be altered by the addition of isotopically light cement during burial diagenesis. If the sediments analysed were affected substantially by burial diagenesis, a strong positive correlation between oxygen and carbon-isotope values should have resulted (Jenkyns and Clayton, 1986; Jenkyns, 1996). The low positive correlation (Fig. 8B) observed between $\delta^{18}O$ and $\delta^{13}C$ at Blieux suggests that the carbon-isotope compositions were not significantly altered during burial diagenesis. Crumière (1991) has shown that, in this part of the Vocontian Basin, the Lower Cenomanian interval has been buried up to 500 m, indicating that the Blieux section has not been subject to deep burial and severe diagenetic alteration. Thierstein and Roth (1991) demonstrated on Lower Cretaceous sediments that the best-preserved nannofossil assemblages and the smallest proportion of diagenetic microcarbonate are found in samples with carbonate contents of between 40 and 60%. With increasing carbonate content, the proportion of microcarbonate gradually increases, the nannofossils show strong signs of calcite overgrowth, and both carbon and oxygen isotopic ratios become more negative. Indeed, Blieux samples with the highest carbonate content (>60%) are characterized by the lowest absolute abundance of nannofossils (Fig. 8A). However, samples with $CaCO_3$ > 60% generally yield heavier carbon- and oxygen-isotope values (Fig. 8B), which is opposite to the expected diagenetic trend. Consequently, these observations support a primary nature for the isotopic values of carbon in the Blieux section.

5.2. Sequence-stratigraphic interpretation

The Mid-Cenomanian was characterized by high-amplitude and high-frequency sea-level changes (Gale, 2000; Gale et al., 2002), but no significant emergent surfaces have been described for that time on the Provence Platform (Crumière, 1991). Accommodation was probably sufficiently high to produce carbonates even during

sea-level lowstand conditions. Platform-derived carbonate settled in the Vocontian Basin during such lowstands, when export was favoured. Consequently, the calcareous bundles described in the section studied are interpreted as LSDs. During late transgressive, maximum-flooding, and early highstand conditions, high carbonate production in shallow-marine environments and low siliciclastic input in the basin (Colombié and Strasser, 2003) led to the formation of the thin calcareous intervals corresponding to MFZs. The marly intervals located below and above the thin calcareous intervals developed when export or carbonate production were low and are interpreted as TDs and HSDs, respectively (Fig. 2). As outlined above (part 4.1.2.), bundles 1 and 4 correspond to large-scale LSDs, the sandy limestone beds at their tops indicating the end of regression. An SB corresponds to a change from a more marly to a more calcareous interval whereas a TS coincides with a change from more calcareous to more marly intervals. Slumps, which usually develop in transgressive deposits, do not systematically form above TSs in the studied section. They occur in LSDs and HSDs as well and may originate from slope destabilization because of high rates of sedimentation, seismic activity or storm and wave action for example (Stow et al., 1996, p. 407; Flügel, 2004, p. 779, and references therein).

5.3. Stratigraphical correlation and cyclostratigraphic interpretation

For the Cenomanian stage of the Anglo-Paris Basin (Gale, 1990) and Western Europe (Gale, 1995), a letter was assigned to each group of couplets (A–E) and each couplet therein was sequentially numbered (for example, from B1 to B45; Fig. 9). In the Cenomanian series of the Anglo-Paris Basin, Robaszynski et al. (1998) demonstrated the existence of five sequences and the lower part of a sixth sequence. Sequence 3 of Robaszynski et al. (1998) corresponds approximately to sequence 2 of Gale (1990, 1995; Fig. 9). In the Lower Saxony Basin, Wilmsen (2003) also recognized five complete depositional sequences (DS Ce I–I to Ce I–V) and the lower part of a sixth (DS Ce VI). The bases of these sequences are interpreted as sequence boundaries; for instance, sequence DS Ce III (i.e., sequence 3 sensu Robaszynski et al., 1998) begins with a third-order sequence boundary SB Ce II and ends with SB Ce III (Wilmsen, 2003; Fig. 9). The latter sequence approximately corresponds to the M. dixoni Zone. Consequently, the second large-scale sequence defined in the Blieux section, which also coincides with the M. dixoni Zone, corresponds approximately to sequence 2 of Gale (1995), sequence 3 of Robaszynski et al. (1998) and sequence DS Ce III of Wilmsen (2003). The M. dixoni Zone lasted 1.6 my (Ogg et al., 2004). According to these authors, the duration of the second large-scale sequence of the Blieux section would be 1.6 my. This sequence includes four medium-scale sequences (Figs. 2 and 9), each of which would have lasted 400 ky, corresponding to the long eccentricity cycle (Strasser et al., 2006).

The interval studied in the Blieux section, from the uppermost part of the M. mantelli Zone to the lower part of the A. rhotomagense Zone, is subdivided into seven complete medium-scale sequences (400 ky); thus, its duration is estimated to be 2.8 my. Lastly, this study indicates that the long (400 ky) eccentricity cycles defined in the Blieux section correlate across western Europe from one basin to the other. However, it seems that the sequence defined in the middle part of the interval studied in the other western European basins (i.e., sequence 2 of Gale, 1995; sequence 3 of Robaszynski et al., 1998; and DS Ce III of Wilmsen, 2003) corresponds to a large-scale sequence in the Blieux section, whereas the one defined in the upper part (above the boundary between the M. dixoni and M. rhotomagense zones) coincides with a medium-scale sequence. Consequently, the attribution of an order to the observed depositional sequences depends
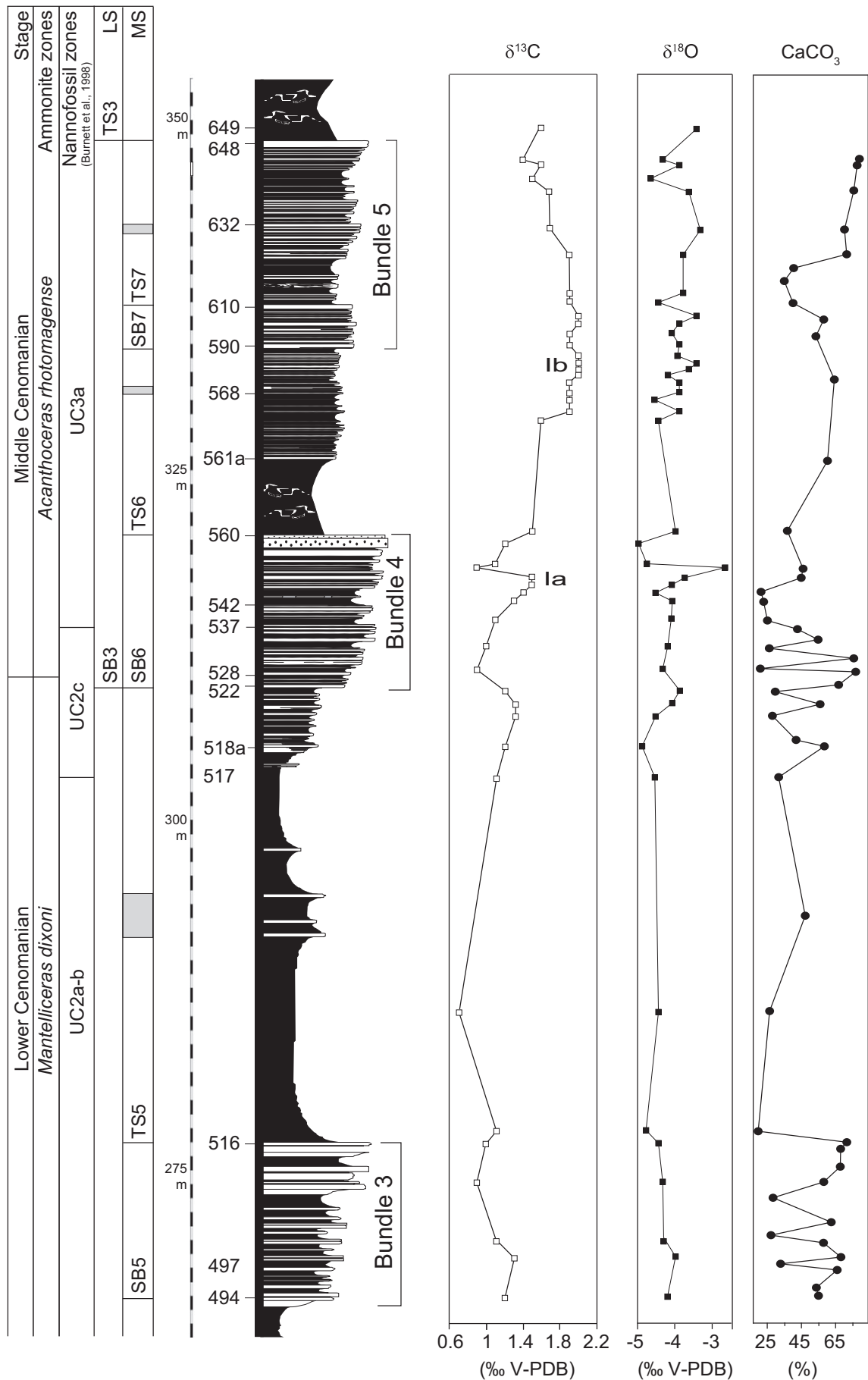
Fig. 7. Carbon and oxygen isotope and calcium carbonate curves plotted against the lithology for a restricted interval (bundles 3–5) for the Blieux section. Ammonite and calcareous nannofossil zonations are represented. LS, Large Scale (3rd order); MS, Medium Scale (400 ky); SB, Sequence Boundary; TS, Transgressive Surface; grey square, Maximum-Flooding Zone; Ia, MCE Ia; Ib, MCE Ib; VPDB, Vienna Pee Dee belemnite.
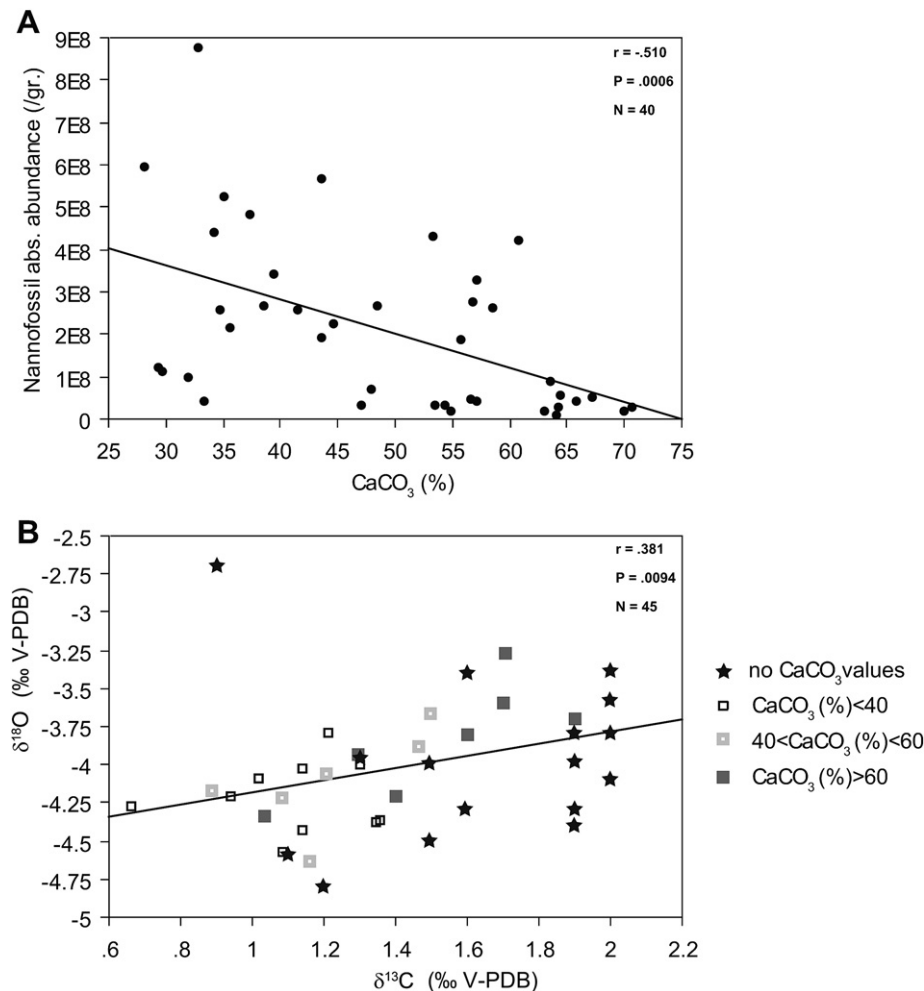
Fig. 8. Bivariate plots showing the relationship between A, calcium carbonate content and absolute abundances of calcareous nannofossils; B, carbon and oxygen isotopes for different classes of calcium carbonate content. Abbreviations: r, coefficient of correlation; P, probability; N, number of measurements.

on the available data and on their interpretation (Strasser et al., 2000; Gale et al., 2002). If this resolution is low (as in the lower and middle part of the interval studied), large-scale sequences are defined while a high resolution (as in the upper part of the interval) leads to the recognition of medium-scale sequences.

6. Discussion

6.1. Inter-basin correlations

In this paper, some classical sections of northwest Europe (Southerham and Folkestone in England, Cap Blanc-Nez in France,

and Baddeckenstedt and Wunstorf in Germany) are correlated using biological events, depositional sequences, stable isotopes and cyclostratigraphy defined in part by previous authors (Gale, 1990, 1995; Amédro et al., 1994, 1997; Paul et al., 1994; Mitchell et al., 1996; Juignet, 1997; Mitchell and Carr, 1998; Robaszynski et al., 1998; Amédro and Robaszynski, 1999; Wilmsen and Niebuhr, 2002; Wilmsen, 2003, 2007; Wilmsen et al., 2007; Wilmsen and Rabe, 2008; Fig. 9). In spite of important thickness variations between the sections and the great distances between them, the lithologies and fossil contents are relatively similar. The ammonoid zonations established by these authors are maintained. In ascending order, the lithological and palaeontological events are (Fig. 9): Sponge Beds,

Fig. 9. Detailed correlations between the Blieux section and the classical sections of northwest Europe (Southerham, Folkestone, Cap Blanc-Nez, Baddeckenstedt and Wunstorf; the numbering of some layers has been changed and sometimes completed; the latter are indicated by numbers in italics). The Southerham section (Sussex, England): Paul et al. (1994) for lithology, carbon-isotope curve, palaeontological data and zonation from B33 to C13; Gale (1990) for lithology from B11 to B36 and B39 to C15; Gale (1995) for lithology and zonation from B1 to B24; Wilmsen (2007) for carbon-isotope curve from B11 to C15. The Folkestone section (Kent, England): Gale (1989) for lithology, palaeontological data and zonation from B1 to C5; Paul et al. (1994) for lithology, carbon-isotope curve, palaeontological data and zonation from B32 to C12; Mitchell and Carr (1998) for lithology from B31 to C2; Robaszynski et al. (1998) for sequence stratigraphy and zonation from B1 to C13. The Cap Blanc-Nez section (= Escalles; Boulonnais, France): Paul et al. (1994) for lithology and isotope curve from B33 to C10; Amédro et al. (1994) for lithology and palaeontological data from B31 to C17; Robaszynski et al. (1998) for sequence stratigraphy and palaeontological data; Amédro and Robaszynski (1999) for lithology, palaeontological data and zonation from B1 to C16. The Baddeckenstedt (Lower Saxony, Germany): Wilmsen and Niebuhr (2002) for lithology, carbon-isotope curve, palaeontological data and zonation; Wilmsen (2003) for sequence stratigraphy; Wilmsen (2007) for carbon-isotope curve; Gale (1995) for numbering from B1 to B24. The Wunstorf section (Lower Saxony, Germany): Mitchell et al. (1996) for lithology from C1a to C1e and carbon-isotope curve from B38 to C2; Wilmsen (2003, 2007), Wilmsen and Niebuhr (2002), and Wilmsen et al. (2007) for lithology, carbon-isotope curve, sequence stratigraphy, palaeontological data and zonation. The lithological and palaeontological events are: I. c., Inoceramus crippsi Event; LSB and USB, Lower and Upper Sponge Beds, respectively; Mar Ev, Mariella Event, The Rib (limestone of couplet B11 of Gale, 1995); I. v., Inoceramus virgatus Event; O. m. 1, 2, 3, Lower, Middle, Upper Orbirhynchia mantelliana Band, respectively; M Ia, Ib, II, III, Marker Marls; DLB, Double Limestone Bed (equivalent to couplets B23–B24); T. s., Turrilites scheuchzerianus Event; L. a., Lyropecten arlesiensis Bed (marl of the couplet B41); 1st C. i., First Cunningtoniceras inerme; 1st C. c., First Cunningtoniceras cunningtoni; P. p., Praeactinocamax primus Event; NL, Nodular Limestones; MCE, Mid-Cenomanian Event (sensu Ernst et al., 1983); P/B, Planktic/Benthic break; S. b., Sciponoceras baculoides; Pyc., Pycnodonte Event.

Mariella Event, The Rib (limestone of couplet B11 of Gale, 1995), *Schloenbachia/Inoceramus virgatus* Event, *Orbirhynchia/Schloenbachia* Event (= Lower *Orbirhynchia* Band), Marl M III, Double Limestone Bed (equivalent to couplets B23–B24), Marl M II, *Turrilites scheuchzerianus* Event, Marl M Ib, Marl M Ia, Middle *Orbirhynchia* Band, *arlesiensis* Bed (marl of the couplet B41), *Praeactinocamax primus* Event, Upper *Orbirhynchia* Band, Mid-Cenomanian Event (MCE sensu Ernst et al., 1983), *Inoceramus atlanticus* Event, and *Pycnodonte* Event (Ernst et al., 1983; Gale, 1995; Wilmsen and Niebuhr, 2002; Wilmsen, 2003, 2007; Wilmsen et al., 2007 and references therein). The cyclostratigraphic analysis at the couplet scale of Gale (1990, 1995) is indicated (couplets B1–B38, *M. dixoni* Zone; B38–B45, C1–C46, *A. rhotomagense* Zone and the lower part of *A. jukesbrownei* Zone). The numbering of some layers has been changed and sometimes completed (Fig. 9, numbers in italics).

To our knowledge, the only attempt at correlation between sections of the Vocontian and northwest Europe basins for the Lower and Middle Cenomanian was that of Gale (1995), which was only based on cyclostratigraphy. Three complementary approaches are used herein to correlate the Blieux section with other northwest European sections: ammonoid biostratigraphy, sequence stratigraphy and chemostratigraphy. When correlations are doubtful, they are indicated by question marks (Fig. 9).

The base of the *M. dixoni* Zone corresponds to the couplet B1 in the northwest European sections (Gale, 1995). The base of this couplet corresponds to a TS recognized in the Anglo-Paris and Lower Saxony basins (Fig. 9, base of TST 3; Robaszynski et al., 1998; Wilmsen, 2003). In the Blieux section, the base of the *M. dixoni* Zone is placed at the base of layer 354 within bundle 1 (Fig. 9). The third-order TS recognized at the top of bundle 1 (layer 422g) can be correlated with the TS (base of TST3) of the Anglo-Paris and Lower Saxony basins. In the Lower Saxony Basin this TS is superposed by the SB Ce II (Wilmsen, 2003). Consequently, SB Ce II can be correlated with the third-order SB2 of the Blieux section.

The MFS of sequence 3 (Robaszynski et al., 1998) is defined at the base of couplet B26 in the Anglo-Paris Basin. The Double Limestone Bed (DLB) B23–B24, which represents a supra-regional marker in northwest Europe (Gale, 1995; Wilmsen, 2007), is located just below this MFS (Fig. 9). This DLB can be correlated with layers 508–516 located at the top of bundle 3 in the Blieux section; this interval represents the third-order MFZ2 and its upper surface can be correlated with the MFS of sequence 3 of the Anglo-Paris Basin (Fig. 9). Above the MFS of sequence 3, *Turrilites scheuchzerianus* occurs in couplets B26 and B28 in the Southerham section, B27–B29 in the Boulonnais, and in B25 in the Lower Saxony Basin (Robaszynski et al., 1998; Wilmsen, 2007). In the Blieux section, this species is also recognized in an interval located above MFZ2 (Fig. 9).

The stratigraphic interval (from B34 to B43) located above SB4 in the Anglo-Paris Basin and SB Ce III in the Lower Saxony Basin is characterized by the appearance of *C. inerme*, which is the index-species of the first zone of the Middle Cenomanian, and the first positive excursion of $\delta^{13}C$ (MCE Ia; Robaszynski et al., 1998; Wilmsen, 2007). The chronological succession of these markers is also identified in bundle 4 of the Blieux section above SB3.

The base of couplet C1 represents the onlap surface of Cenomanian sequence 4 (Southerham, Folkestone and Cap Blanc-Nez sections; Fig. 9) according to Gale (1995), Mitchell et al. (1996), Mitchell and Carr (1998), and Robaszynski et al. (1998). This TS is correlated with the medium scale TS (TS6) recognized at the top of bundle 4 in the Blieux section. The transgression is characterized in both the Anglo-Paris and Vocontian basins by a sharp lithological change, which is also recognized in the Wunstorf section (Fig. 9). Although the sequential interpretation proposed by Wilmsen (2003, 2007) is different for this part, the surface corresponding to the lithological change is used to establish correlations between

the three basins and is used as a datum. Above, the second positive carbon-isotope trend (MCE Ib; Paul et al., 1994; Gale, 1995; Mitchell et al., 1996) occurs, which is also used to establish the correlations. Above this second trend, correlations between the different basins can be established using the abundance of the orthocone *S. baculoides* recognized in all of the sections (Robaszynski et al., 1998; Wilmsen, 2003; see 4.2.2.). The first occurrence of this species seems concomitant to this positive trend or excursion in some sections (Fig. 9).

6.2. The "mid-Cenomanian event"

This event was first defined by Paul et al. (1994) as a carbon-isotope excursion ($\delta^{13}C$) characterized by two positive peaks (MCE Ia, MCE Ib; Mitchell et al., 1996). This compares well with the Cenomanian/Turonian Boundary Event (CTBE) excursion, which is also characterized by two positive peaks in the $\delta^{13}C$ curves (Schlanger et al., 1987; Arthur et al., 1988; Gale et al., 1993; Erbacher et al., 2005). CTBE corresponds to OAE 2, which is the most prominent and widespread Cretaceous "Oceanic Anoxic Event" (OAE; Schlanger and Jenkyns, 1976; Jenkyns, 1980; Arthur et al., 1990). OAEs are associated with major excursions of $\delta^{13}C$ in various carbon reservoirs. Positive carbon-isotope excursions MCE Ia and MCE Ib are recorded in marine carbonates (in England and northern France: Jenkyns et al., 1994; Paul et al., 1994; Mitchell et al., 1996; Jarvis et al., 2001, 2006; southeastern France: this study; Spain: Rodriguez-Lazaro et al., 1998; Stoll and Schrag, 2000; Italy: Stoll and Schrag, 2000; northern Germany: Mitchell et al., 1996; Wilmsen, 2007; Morocco: Gertsch et al., 2010; western North Atlantic: Ando et al., 2009), in marine organic carbon (tropical Atlantic Ocean: Friedrich et al., 2009; Morocco: Gertsch et al., 2010), and in terrestrial organic matter (Japan: Uramoto et al., 2007). OAEs are distributed world-wide and correspond to organic-rich deposits (black shales). As OAEs, MCE I is world-wide (references cited above) but in contrast to OAEs, it is characterized by laminated black shales only in the tropical Atlantic Ocean (Demerara Rise, ODP Leg 207, TOC values from 5 to 18%; Friedrich et al., 2009). Laminated dark marls are recognized in two sections of the Vocontian Basin (Vergons and St Lions sections; Gale, 1995), but not in the Blieux section studied, and laminated shales are identified in Morocco (Azazoul Road section; Gertsch et al., 2010), but TOC values are not available. In the Mohammed Plage section (Tarfaya Basin, southwest Morocco), the TOC values fluctuate around 5% in the sediments corresponding to MCE I but these sediments are not black shales (Kuhnt et al., 2009).

Long-term positive excursions in the $\delta^{13}C$ of marine and terrestrial organic carbon are thought to result from global burial of ^{12}C-enriched organic matter (e.g., Arthur et al., 1988). A long-term positive trend is recognized from MCE I up to the CTBE, but how can the two small positive carbon-isotope peaks corresponding to MCE I be explained? Rapid sea-level fluctuations ("up to 1 my"; Mitchell et al., 1996) are probably the reason. The long eccentricity (400 ky) cycle is recognized as the main factor controlling the formation of the Cenomanian depositional sequences (Gale et al., 2002, 2008). In the Blieux section, the first positive excursion (MCE Ia) is observed in the middle of the LSD of a medium-scale sequence (400 ky), and the second positive trend (MCE Ib) begins at the end of the TD of the same sequence. Consequently, the duration of MCE I is less than 400 ky. Correlation between carbon-isotope excursions and eustatic sequences was established in the Anglo-Paris Basin by Mitchell et al. (1996), who recognized that MCE Ia and MCE Ib occur in the LSD and TD, respectively. These authors proposed that changes in the carbon cycle are associated with rapid regressive–transgressive cycles, leading to the same response of the carbon system during LSDs and TDs. Transgressive intervals are generally recognized as intervals during which there is
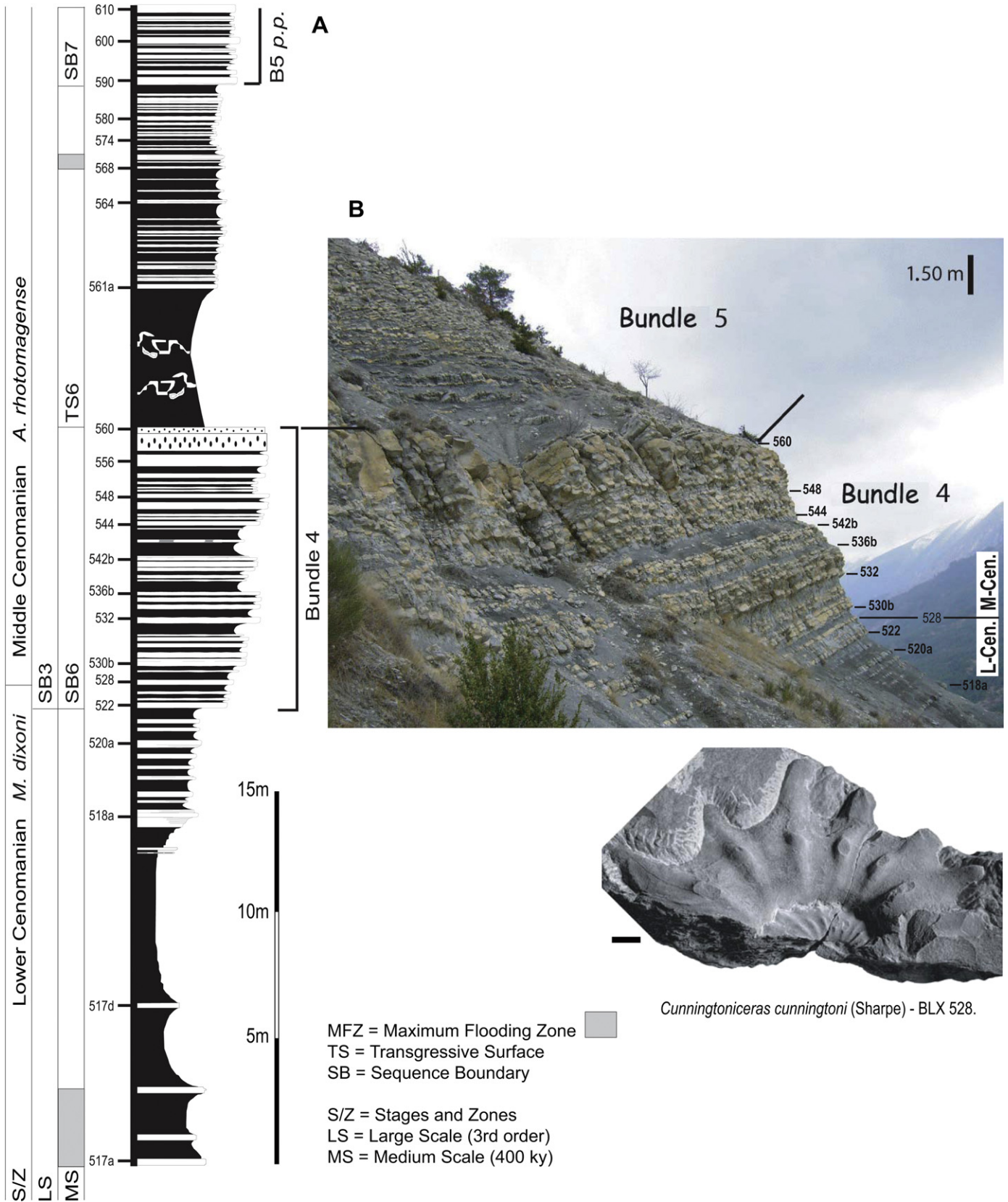
Fig. 10. A, detailed lithological column around the Lower/Middle Cenomanian boundary (L-Cen./M-Cen.) of the Blieux section proposed as candidate for a Global Boundary Stratotype Section and Point (GSSP) of the Middle Cenomanian Substage. B, photograph of the Blieux section showing bundle 4 in which the boundary is placed. C, photograph of a specimen of *Cunningtoniceras cunningtoni* (Sharpe), FSL 338302, BLX 528, *A. rhotomagense* Zone. Scale bar represents 1 cm.

an increased flux of nutrients leading to an increase in primary productivity and enhanced ^{12}C-enriched marine organic-carbon burial rates and elevated δ^{13}C values in ocean waters recorded in biogenic carbonates. Positive carbon-isotope excursions during sea-level falls are a result of increased incorporation of organic carbon in soils and biota associated with soil formation on exposed continental shelves.

Gale et al. (2002, 2008) have proposed that rapid sea-level changes (400 ky) have a glacioeustatic origin for the Cenomanian. The glaciation hypothesis has been advanced by Stoll and Schrag (2000) and Miller et al. (2003, 2005). Several authors have suggested a cool climate mode in western Europe during MCE I, supported by two southward incursions of Boreal nektonic-benthic taxa into European shelf seas: the first at the onset of the first carbon-isotope excursion and the second within the δ^{13}C maximum of the second excursion (Paul et al., 1994; Gale, 1995; Wilmsen, 2003). On the basis of brachiopod oxygen-isotope data, Voigt et al. (2004) have demonstrated that a cooling event (2–3 °C) coincides with MCE I on European shelves. However, recent stable isotope data both from tropical Atlantic Ocean and western North Atlantic argue against a mid-Cenomanian glaciation event (Moriya et al., 2007; Ando et al., 2009).

All of this information shows that (1) MCE Ia and MCE Ib are recorded in various carbon reservoirs and are recognized worldwide (as OAEs): thus, both ocean and atmosphere reservoirs were affected by the perturbation in the carbon cycle; (2) MCE I is not characterized by the occurrence of black shales (only recognized in one drilled ODP Atlantic Site); (3) MCE Ia and MCE Ib are associated with rapid sea-level changes, possibly of glacioeustatic origin.

6.3. The Blieux section: candidate for a Global Boundary Stratotype Section and Point (GSSP) of the Middle Cenomanian Substage

The Southerham section (Gray Quarry, Sussex, England) has been proposed as a reference section for the Lower/Middle Cenomanian boundary (Tröger and Kennedy, 1996; see also Ogg et al., 2004). This section was studied for lithostratigraphy (Lake et al., 1987), cyclostratigraphy (Gale, 1990, 1995), macrofauna (Paul et al., 1994), carbon and oxygen stable isotopes (Paul et al., 1994; Wilmsen, 2007), and Total Organic Carbon (Paul et al., 1994). Paul et al. (1994) emphasized that "it has the unique advantage of yielding ammonites across an expanded Early/Middle Cenomanian boundary". However, in the lower part of the Middle Cenomanian, some levels are condensed (B42–B43; C1–C2; Paul et al., 1994) or absent (B44–B45; Gale, 1995). Moreover, micropalaeontological data are not available for this section, and sequence stratigraphy has been determined for the Kent (England) but not for the Sussex sections (Robaszynski et al., 1998).

The Blieux section has several advantages as a good candidate for the GSSP of the Middle Cenomanian. It is easily accessible (close to a road) and in its natural state, unaffected by development. The outcrop conditions are good throughout the succession. This hemipelagic section is more expanded than the sections of the Anglo-Paris and Lower Saxony basins and ammonoids are relatively common to abundant, with *Cunningtoniceras* being present. According to the proposal made previously (see 4.2.2.), the "golden spike" of the Middle Cenomanian GSSP could be placed at the base of the layer 528 in the Blieux section where the genus *Cunningtoniceras* appears (Figs. 3 and 10). The Lower/Middle Cenomanian boundary is also well characterized by the recognition of the nannofossil Subzone UC2C (from layers 517d to 537) of Burnett et al. (1998; Fig. 7). Seven metres above the boundary, the first δ^{13}C positive excursion (MCE Ia) occurs (Fig. 7). The base of bundle 4, beginning three layers below the Lower/Middle Cenomanian boundary, is interpreted as both a medium-scale (400 ky) and a large-scale (3rd order) sequence boundary. The third-order SB of

the Blieux section (SB3) corresponds to the third-order Ce3 defined in Hardenbol et al. (1998) and figured in Ogg et al. (2004).

7. Conclusions

The integrated study (ammonoids, calcareous nannofossils, carbon and oxygen stable isotopes, sequence stratigraphy) of the Lower–Middle Cenomanian of the Blieux section of southeast France has led to five major results:

1. Concerning the ammonoid zonal scheme, the *M. dixoni* and the *A. rhotomagense* zones have been identified. The appearance of the genus *Cunningtoniceras* (*C. inerme* or *C. cunningtoni*) is used to place the base of the *A. rhotomagense* Zone and thus the base of the Middle Cenomanian; it corresponds to layer 528 in the Blieux section. The Lower/Middle Cenomanian boundary is also well characterized by the recognition of the nannofossil Subzone UC2C (from layers 517d to 537) of Burnett et al. (1998).

2. A sequence-stratigraphic analysis is proposed for the Blieux section and two orders of depositional sequences have been recognized: medium-scale (400 ky) and large-scale (third order). The duration of the interval studied from the top of the *M. mantelli* Zone to the lower part of the *A. rhotomagense* Zone can be estimated to be 2.8 my (seven complete medium-scale sequences). SB3 of the Blieux section, located just below the Lower/Middle Cenomanian boundary, corresponds to the third-order SB Ce3 defined in Hardenbol et al. (1998).

3. The marked positive excursion of δ^{13}C in the lower part of the *A. rhotomagense* Zone (upper part of bundle 4) corresponds to Middle Cenomanian event Ia. A second increase observed below bundle 5, showing a plateau rather than a peak, corresponds to Middle Cenomanian event Ib. The duration of MCE I is less than 400 ky.

4. Detailed correlations between the hemipelagic part of the subtropical Vocontian Basin and the mid-latitude shelf-sea of the Anglo-Paris and Lower Saxony basins are proposed for the Early and Middle Cenomanian.

5. This integrated study allows us to propose the Blieux section as a good candidate for the GSSP of the Middle Cenomanian. The "golden spike" of this substage could be placed at the first appearance of the genus *Cunningtoniceras*, corresponding to layer 528.

References

Amédro, F., Robaszynski, F., 1999. Les craies cénomaniennes du Boulonnais. Comparaison avec l'Aube (France) et le Kent (Royaume Uni). Géologie de la France 2, 33–53.

Amédro, F., Robaszynski, F., Colleté, C., Fricot, C., 1997. Les craies du Cénomanien-Turonien de l'Aube et du Boulonnaies: des événements litho- et bio-sédimentaires communs. Annales de la Société Géologique du Nord 5, 189–197.

Amédro, F., Colleté, C., Fricot, C., Robaszynski, F., 1994. Extension inter-régionale de niveaux-repères dans les craies cénomaniennes du bassin anglo-parisien (Boulonnais, Aube, Kent). Bulletin d'Information des Géologues du Bassin de Paris 31, 3–8.

Ando, A., Huber, B.T., MacLeod, K.G., Ohta, T., Khim, B.-K., 2009. Blake Nose stable isotopic evidence against the mid-Cenomanian glaciation hypothesis. Geology 37, 451–454.

Arthur, M.A., Dean, W.E., Pratt, L.M., 1988. Geochemical and climatic effects of increased organic carbon burial at the Cenomanian/Turonian boundary. Nature 335, 714–717.

Arthur, M.A., Jenkyns, H.C., Brumsack, H.J., Schlanger, S.O., 1990. Stratigraphy, geochemistry and paleoceanography of organic carbon-rich Cretaceous sequences. In: Ginsburg, R.N., Beaudoin, B. (Eds.), Cretaceous Resources, Events and Rhythms. NATO ASI Series C, 304. Springer-Verlag, Berlin, pp. 75–119.

Beaufort, L., 1991. Adaptation of the random settling method for quantitative studies of calcareous nannofossils. Micropalaeontology 37, 415–418.

Boule, M., Lemoine, P., Thévenin, A., 1906. Paléontologie de Madagascar 3. Céphalopodes crétacés des environs de Diego-Suarez. Annales de Paléontologie 1, 1–76.

Bréhéret, J.G., 1997. L'Aptien et l'Albien de la fosse vocontienne (des bordures au bassin). Evolution de la sédimentation et enseignements sur les événements anoxiques. Publication de la Société Géologique du Nord 25, 1–614.

Briais, J., 2010. Paléogéographie du bassin du Sud-Est de la France au Crétacé post-Urgonien. Unpublished Master's thesis 2, Claude Bernard University of Lyon 1, 51 pp.

Burnett, J.A., Gallagher, L.T., Hampton, M.J., 1998. Upper Cretaceous. In: Bown, P.R. (Ed.), Calcareous Nannofossil Biostratigraphy. British Micropalaeontological Society, Publications Series. Chapman and Hall/Kluwer Academic Publishers, pp. 132–199.

Carpentier, A., 2007. Changements paléocéanographiques au cours du Cénomanien: réponse du plancton calcaire. Unpublished Master's thesis 2, Université Claude Bernard Lyon 1, 47 pp.

Catuneanu, O., Abreu, V., Bhattacharya, J.P., Blum, M.D., Dalrymple, R.W., Eriksson, P.G., Fielding, C.R., Fisher, W.L., Galloway, W.E., Gibling, M.R., Giles, K.A., Holbrook, J.M., Jordan, R., Kendall, C.G.St.C., Macurda, B., Martinsen, O.J., Miall, A.D., Neal, J.E., Nummedal, D., Pomar, L., Posamentier, H.W., Pratt, B.R., Sarg, J.F., Shanley, K.W., Steel, R.J., Strasser, A., Tucker, M.E., Winker, C., 2009. Towards the standardization of sequence stratigraphy. Earth-Science Reviews 92, 1–33.

Collignon, M., 1964. Atlas des fossiles caractéristiques de Madagascar (Ammonites). Cénomanien. Mémoires du Service Géologique, Tananarive 11. 1–151.

Colombié, C., Strasser, A., 2003. Depositional sequences in the Kimmeridgian of the Vocontian Basin (France) controlled by carbonate export from shallow-water platforms. Geobios 36, 675–683.

Conard, M., 1983. La dynamique des dépôts cénomaniens de Haute-Provence: observations nouvelles et implications paléogéographiques. Bulletin de la Société Géologique de France 7 (25), 239–246.

Cooper, M.R., 1994. Towards a phylogenetic classification of the Cretaceous ammonites. III. Scaphitaceae. Neues Jahrbuch für Geologie und Paläontologie 193, 165–193.

Cooper, M.R., 1998. A revision of the Turrilitidae (Cretaceous Ammonoidea) from the Cambridge Greensand. Neues Jahrbuch für Geologie und Paläontologie 207, 145–170.

Cooper, M.R., 1999. Towards a phylogenetic classification of the Cretaceous ammonites. VII. Turrilitidae. Neues Jahrbuch für Geologie und Paläontologie 213, 1–18.

Cotillon, P., 1971. Le Crétacé inférieur de l'Arc subalpin de Castellane entre l'Asse et le Var. Stratigraphie et sédimentologie. Mémoires du Bureau de Recherches Géologiques et Minières 68, 1–313.

Crumière, J.P., 1989. Crise anoxique à la limite Cénomanian–Turonian dans le bassin subalpin oriental (Sud-Est de la France). Relation avec l'eustatisme. Geobios 22, 189–203.

Crumière, J.P., 1991. 1- The Cenomanian–Turonian Oceanic Anoxic Event (C.T.O.A.E.) in the Southern Subalpine Domain (northwestern Tethyan margin, south-east of France). In: Crumière, J.P., Cotillon, P., Schaaf (Coord.), A. (Eds.), Cenomanian–Turonian Boundary Events. Excursion post-colloque dans le Sud-Est de la France, Livret Guide, pp. 9–56.

Erbacher, J., Friedrich, O., Wilson, P.A., Birch, H., Mutterlose, J., 2005. Stable organic carbon isotope stratigraphy across Oceanic Anoxic Event 2 of Demerara Rise, western tropical Atlantic. Geochemistry, Geophysics, Geosystems 6, Q06010. http://dx.doi.org/10.1029/2004GC000850.

Erbacher, J., Thurow, J., 1997. Influence of oceanic anoxic events on the evolution of mid-Cretaceous radiolaria in the North Atlantic and western Tethys. Marine Micropaleontology 30, 139–158.

Erbacher, J., Thurow, J., Littke, R., 1996. Evolution patterns of radiolaria and organic matter variations: a new approach to identify sea-level changes in mid-Cretaceous pelagic environments. Geology 24, 499–502.

Ernst, G., Schmid, F., Seibertz, E., 1983. Event-stratigraphie im Cenoman und Turon von NW-Deutschland. Zitteliana 10, 531–554.

Fernando, A.G.S., Takashima, R., Nishi, H., Giraud, F., Okada, H., 2010. Calcareous nannofossil biostratigraphy of the Thomel Level (OAE2) in the Lambruisse section, Vocontian Basin, southeast France. Geobios 43, 45–57.

Ferry, S., Rubino, J.L., 1989. Mesozoic Eustacy Record on Western Tethyan Margins. Guide-book of the post-meeting field trip in the Vocontian Trough, 25th–28th November 1989, 2ème Congrès Français de Sédimentologie, Lyon, 141 pp.

Flügel, E., 2004. Microfacies of Carbonate Rocks: Analysis, Interpretation and Application. Springer-Verlag, Berlin, 976 pp.

Friedrich, O., Erbacher, J., Wilson, P.A., Moriya, K., Mutterlose, J., 2009. Paleoenvironmental changes across the Mid Cenomanian Event in the tropical Atlantic Ocean (Demerara Rise, ODP Leg 207) inferred from benthic foraminiferal assemblages. Marine Micropaleontology 71, 28–40.

Gale, A.S., 1989. Field Meeting at Folkestone Warren, 29th November, 1987. Proceedings of the Geologists' Association 100, 73–82.

Gale, A.S., 1990. A Milankovitch scale for Cenomanian time. Terra Nova 1, 420–425.

Gale, A.S., 1995. Cyclostratigraphy and correlation of the Cenomanian stage in Western Europe. In: House, M.R., Gale, A.S. (Eds.), Orbital Forcing Timescales and Cyclostratigraphy. Geological Society, London, Special Publication 85, pp. 177–197.

Gale, A.S., 2000. The Cretaceous world. In: Culver, S.J., Rawson, P.F. (Eds.), Biotic Response to Global Change: the Last 145 Million Years. The Natural History Museum, London, and Cambridge University Press, Cambridge, pp. 4–19.

Gale, A.S., Hardenbol, J., Hathway, B., Kennedy, W.J., Young, J.R., Phansalkar, V., 2002. Global correlation of Cenomanian (Upper Cretaceous) sequences: evidence for Milankovitch control on sea level. Geology 30, 291–294.

Gale, A.S., Jenkyns, H.C., Kennedy, W.J., Corfield, R.M., 1993. Chemostratigraphy versus biostratigraphy: data from around the Cenomanian-Turonian boundary. Journal of the Geological Society, London 150, 29–32.

Gale, A.S., Kennedy, W.J., Burnett, J.A., Caron, M., Kidd, B.E., 1996. The Late Albian to Early Cenomanian succession at Mont Risou near Rosans (Drôme, SE France): an integrated study (ammonites, inoceramids, planktonic foraminifera, nanno-fossils, oxygen and carbon isotopes). Cretaceous Research 17, 515–606.

Gale, A.S., Voigt, S., Sageman, B.B., Kennedy, W.J., 2008. Eustatic sea-level record for the Cenomanian (Late Cretaceous) – extension to the Western Interior Basin, USA. Geology 36, 859–862.

Geisen, M., Bollmann, J., Herrle, J.O., Mutterlose, J., Young, J.R., 1999. Calibration of the random settling technique for calculation of absolute abundances of calcareous nannoplankton. Micropalaeontology 45, 437–442.

Gertsch, B., Adatte, T., Keller, G., Tantawy, A.A.A.M., Berner, Z., Mort, H.P., Fleitmann, D., 2010. Middle and late Cenomanian oceanic anoxic events in shallow and deeper shelf environments of western Morocco. Sedimentology 57, 1430–1462.

Giraud, F., Olivero, D., Baudin, F., Reboulet, S., Pittet, B., Proux, O., 2003. Minor changes in surface water fertility across the Oceanic Anoxic Event 1d (latest Albian, SE France) evidenced by calcareous nannofossils. International Journal of Earth Sciences 92, 267–284.

Giraud, F., Reboulet, S., Carpentier, A., 2008. The mid-Cenomanian event in southeastern France: evidence from geochemical and paleontological data. Réunions Thématiques du GFC «Les climats du Crétacé», 1–2 Décembre 2008, Paris (France), Book of abstracts, pp. 23–24.

Grosheny, D., Malartre, F., 1997. Stratégies adaptatives des foraminifères benthiques et planctoniques à la limite Cénomanien-Turonien dans le bassin du S.E. de la France: essai de compréhension globale. Geobios 21, 181–193.

Grosheny, D., Beaudoin, B., Morel, L., Desmares, D., 2006. High-resolution biostratigraphy and chemostratigraphy of the Cenomanian/Turonian boundary event in the Vocontian Basin, southeast France. Cretaceous Research 27, 629–640.

Haq, B.U., Hardenbol, J., Vail, P.R., 1987. Chronology of fluctuating sea levels since the Triassic (250 million years ago to present). Science 235, 1156–1166.

Hardenbol, J., Thierry, J., Farley, M.B., Jacquin, T., de Graciansky, P.C., Vail, P.R., 1998. Mesozoic and Cenozoic sequence chronostratigraphic framework in European basins. In: de Graciansky, P.C., Hardenbol, J., Jacquin, T., Vail, P.R. (Eds.), 1998. Mesozoic and Cenozoic Sequence Stratigraphy of European Basins. SEPM (Society for Sedimentary Geology), Special Publication 60, pp. 3–13.

Immenhauser, A., Holmden, C., Patterson, W.P., 2008. Interpreting the carbon-isotope record of ancient shallow epeiric seas: lessons from the recent. In: Homden, C. (Ed.), 2008. Dynamics of Epeiric Seas. Geological Association of Canada, Special Paper 48, pp. 137–174.

Jarvis, I., Gale, A.S., Jenkyns, H.C., Pearce, M.A., 2006. Secular variation in Late Cretaceous carbon isotopes: a new $\delta^{13}C$ carbonate reference curve for the Cenomanian–Campanian (99.6–70.6 Ma). Geological Magazine 143, 561–608.

Jarvis, I., Murphy, A.M., Gale, A.S., 2001. Geochemistry of pelagic and hemipelagic carbonates: criteria for identifying systems tracts and sea-level changes. Journal of the Geological Society, London 158, 685–696.

Jenkyns, H.C., 1980. Cretaceous anoxic events: from continents to oceans. Journal of the Geological Society, London 137, 171–188.

Jenkyns, H.C., 1996. Relative sea-level change and carbon isotopes: data from the Upper Jurassic (Oxfordian) of central and southern Europe. Terra Nova 8, 75–85.

Jenkyns, H.C., Clayton, C.J., 1986. Black shales and carbon isotopes in pelagic sediments from the Tethyan Lower Jurassic. Sedimentology 33, 87–106.

Jenkyns, H.C., Gale, A.S., Corfield, R.M., 1994. Carbon- and oxygen-isotope stratigraphy of the English Chalk and Italian Scaglia and its palaeoclimatic significance. Geological Magazine 131, 1–34.

Joly, B., 2000. Les Juraphyllitidae, Phylloceratidae, Neophylloceratidae (Phylloceratacedae, Phylloceratina, Ammonoidea) de France au Jurassique et au Crétacé. Mémoire Spéciale Geobios 23 et Mémoire de la Société Géologique de France 174, 1–204.

Juignet, P., 1977. Ammonite faunas from the Cenomanian around Le Mans (Sarthe France). Palaeontological Society of Japan, Special Paper 21, 143–150.

Juignet, P., 1997. La craie: sédimentation et enregistrements stratigraphiques. Apports des méthodes d'études classiques et d'approches nouvelles. Annales de la Société Géologique du Nord 5, 145–158.

Juignet, P., Kennedy, W.J., 1976. Faunes d'Ammonites et biostratigraphie comparée du Cénomanien du nord-ouest de la France (Normandie) et du sud de l'Angleterre. Société Géologique de Normandie et des Amis du Muséum du Havre 63, 1–193.

Kandel, D., 1992. Analyse paléotectonique de la plate-forme méridionale du bassin vocontien et de ses bordures durant l'intervalle barrémo-albien (Ventoux-Lure-Baronnies, chaînes subalpines méridionales, France). Unpublished PhD thesis, University of Paris VI, 323 pp.

Kaplan, U., Kennedy, W.J., Lehmann, J., Marcinowski, R., 1998. Stratigraphie und Ammonitenfaunen des westfälischen Cenoman. Geologie und Paläontologie in Westfalen 51, 1–236.

Kennedy, W.J., 1969. The correlation of the Lower Chalk of South-East England. Proceedings of the Geologists' Association 80, 459–560.

Kennedy, W.J., 1971. Cenomanian ammonites from southern England. The Palaeontological Association, London, Special Papers in Palaeontology 8, 1–133.

Kennedy, W.J., Cobban, W.A., 1976. Aspects of ammonite biology, biogeography, and biostratigraphy. The Palaeontological Association, London, Special Papers in Palaeontology 17, 1–94.

Kennedy, W.J., Hancock, J.M., 1970. Ammonites of the genus Acanthoceras from the Cenomanian of Rouen, France. Palaeontology 13, 462–490.

Kennedy, W.J., Hancock, J.M., 1971. Mantelliceras saxbii, and the horizon of the Martimpreyi Zone in the Cenomanian of England. Palaeontology 14, 437–454.

Kennedy, W.J., Hancock, J.M., Christensen, W.K., 1981. Albian and Cenomanian ammonites from the island of Bornholm (Denmark). Bulletin of the Geological Society of Denmark 29, 203–244.

Kennedy, W.J., Juignet, P., 1975. Répartition des genres et espèces d'ammonites caractéristiques du Cénomanien du Sud de l'Angleterre et de la Normandie. Comptes Rendus de l'Académie des Sciences Paris 280, 1221–1224.

Kennedy, W.J., Juignet, P., 1983. A revision of the ammonite faunas of the type Cenomanian. I. Introduction, Ancyloceratina. Cretaceous Research 4, 3–83.

Kennedy, W.J., Juignet, P., 1984. A revision of the ammonite faunas of the type Cenomanian. 2. The families Binneyitidae, Desmoceratidae, Engonoceratidae, Placenticeratidae, Hoplitidae, Schloenbachiidae, Lyelliceratidae and Forbesiceratidae. Cretaceous Research 5, 93–161.

Kennedy, W.J., Juignet, P., 1993. A revision of the ammonite faunas of the type Cenomanian. 4. Acanthoceratinae (Acompsoceras, Acanthoceras, Protacanthoceras, Cunningtoniceras and Thomelites). Cretaceous Research 14, 145–190.

Kennedy, W.J., Juignet, P., Wright, C.W., 1986. A revision of the ammonite faunas of the type Cenomanian. 3. Mantelliceratinae. Cretaceous Research 7, 19–62.

Kennedy, W.J., Gale, A.S., Bown, P.R., Caron, M., Dovery, R.J., Gröcke, D., Wray, D.S., 2000. Integrated stratigraphy across the Aptian-Albian boundary in the Marnes Bleues, at the Col de Pré-Guittard, Arnayon (Drôme), and at Tartonne (Alpes-de-Haute-Provence), France: a candidate Global Boundary Stratotype Section and Point for the base of the Albian stage. Cretaceous Research 21, 591–720.

Klein, J., Hoffmann, R., Joly, B., Shigeta, Y., Vašíček, Z., 2009. Lower Cretaceous Ammonites IV, Boreophylloceratoidea, Phylloceratoidea, Lytoceratoidea, Tetragonitoidea, Haploceratoidea, including the Upper Cretaceous representatives. In: Riegraf, W. (Ed.), Fossilium Catalogus I: Animalia. Backhuys Publishers (Leiden), Part 146, 416 pp.

Kuhnt, W., Holbourn, A., Gale, A., Chellai, El H., Kennedy, W.J., 2009. Cenomanian sequence stratigraphy and sea-level fluctuations in the Tarfaya Basin (SW Morocco). Geological Society of America, Bulletin 121, 1695–1710.

Lake, R.D., Young, B., Wood, C.J., Mortimore, R.N., 1987. Geology of the Country Around Lewes. Memoirs of the British Geological Survey, 117 pp.

Lees, J.A., 2002. Calcareous nannofossil biogeography illustrates palaeoclimate change in the Late Cretaceous Indian Ocean. Cretaceous Research 23, 537–634.

Lehmann, J., 1998. Systematic palaeontology of the ammonites of the Cenomanian–Lower Turonian (Upper Cretaceous) of northern Westphalia, north Germany. Tübinger Geowissenschaftliche Arbeiten 37, 1–58.

Marcinowski, R., 1980. Cenomanian ammonites from the German Democratic Republic, Poland, and the Soviet Union. Acta Geologica Polonica 30, 215–325.

Masse, J.P., Philip, J., 1976. Paléogéographie et tectonique du Crétacé moyen en Provence: révision du concept d'isthme durancien. Revue de Géographie Physique et Géologie Dynamique 18, 49–66.

Miller, K.G., Sugarman, P.J., Browning, J.V., Kominz, M.A., Hernández, J.C., Olsson, R.K., Wright, J.D., Feigenson, M.D., Van Sickel, W., 2003. Late Cretaceous chronology of large, rapid sea level changes: Glacioeustasy during the greenhouse world. Geology 31, 585–588.

Miller, K.G., Wright, J.D., Browning, J.V., 2005. Visions of ice sheets in a greenhouse world. Marine Geology 217, 215–231.

Mitchell, S.F., Carr, I.T., 1998. Foraminiferal response to mid-Cenomanian (Upper Cretaceous) palaeoceanographic events in the Anglo-Paris Basin (Northwest Europe). Palaeogeography, Palaeoclimatology, Palaeoecology 137, 103–125.

Mitchell, S.F., Paul, C.R.C., Gale, A.S., 1996. Carbon isotopes and sequence stratigraphy. In: Howell, J.A., Aitken, J.F. (Eds.), High Resolution Sequence Stratigraphy: Innovations and Applications. Geological Society, London, Special Publication 104, pp. 11–24.

Mitchum R.M., Jr., Vail, P.R., Thompson S., III, 1977. Seismic stratigraphy and global changes of sea-level, part 2: the depositional sequence as a basic unit for stratigraphic analysis. In: Payton, C.E. (Ed.), Seismic Stratigraphy – Applications to Hydrocarbon Exploration. American Association of Petroleum Geologists, Memoir 26, pp. 53–62.

Monnet, C., 2005. Anisian (Middle Triassic) and Cenomanian (mid-Cretaceous) Ammonoids: Biochronology, Biodiversity, and Evolutionary Trends. Unpublished PhD thesis, University of Zürich, 706 pp.

Monnet, C., Bucher, H., 1999. Biochronologie quantitative (associations unitaires) des faunes d'ammonites du Cénomanien du Sud-Est de la France. Bulletin de la Société Géologique de France 170, 599–610.

Monnet, C., Bucher, H., 2002. Cenomanian (early Late Cretaceous) ammonoid faunas of Western Europe. Part 1: Biochronology (Unitary Associations) and diachronism of datums. Eclogae Geologicae Helvetiae 95, 57–73.

Monnet, C., Bucher, H., 2007. Ammonite-based correlations in the Cenomanian–lower Turonian of north-west Europe, central Tunisia and the Western Interior (North America). Cretaceous Research 28, 1017–1032.

Monnet, C., Bucher, H., Escarguel, G., Guex, J., 2003. Cenomanian (early Late Cretaceous) ammonoid faunas of Western Europe. Part 2: Diversity patterns and the end-Cenomanian anoxic event. Eclogae Geologicae Helvetiae 96, 381–398.

Moriya, K., Wilson, P., Friedrich, O., Erbacher, J., Kawahata, H., 2007. Testing for ice sheets during the mid-Cretaceous greenhouse using glassy foraminiferal calcite from the mid-Cenomanian tropics on Demerara Rise. Geology 35, 615–618.

Ogg, J.G., Agterberg, F.P., Gradstein, F.M., 2004. The Cretaceous period. In: Gradstein, F.M., Ogg, J.G., Smith, A. (Eds.), A Geologic Time Scale 2004. Cambridge University Press, Cambridge, pp. 344–384.

Owen, D., 1996. Interbasinal correlation of the Cenomanian Stage; testing the lateral continuity of sequence boundaries. In: Howell, J.A., Aitken, J.F. (Eds.), High Resolution Sequence Stratigraphy: Innovations and Applications. Geological Society, London, Special Publication 104, pp. 269–293.

Paul, C.R.C., Mitchell, S.F., Marshall, J.D., Leary, P.N., Gale, A.S., Duane, A.M., Ditchfield, P.W., 1994. Palaeoceanographic events in the Middle Cenomanian of Northwest Europe. Cretaceous Research 15, 707–738.

Perch-Nielsen, K., 1985. Mesozoic calcareous nannofossils. In: Bolli, H.M., Saunders, J.B., Perch-Nielsen, K. (Eds.), Plankton Stratigraphy. Cambridge University Press, Cambridge, pp. 17–86.

Philip, J., 1978. Stratigraphie et paléoécologie des formations à rudistes du Cénomanien: l'exemple de la Provence. Géologie Méditerranéenne 5, 155–168.

Posamentier, H.W., Jervey, M.T., Vail, P.R., 1988. Eustatic controls on clastic deposition I – conceptual framework. In: Wilgus, C.K., Hastings, B.S., Kendall, C.G.St.C., Posamentier, H.W., Ross, C.A., Van Wagoner, J.C. (Eds.), Sea Level Changes – An Integrated Approach. Society of Economic Paleontologists and Mineralogists, Special Publication 42, pp. 110–124.

Reboulet, S., Giraud, F., Proux, O., 2005. Ammonoid abundance variations related to changes in trophic conditions across the oceanic anoxic event 1d (latest Albian, SE France). Palaios 20, 121–141.

Renz, O., 1968. Die Ammonoidea im Stratotyp des Vraconnien bei St Croix (Kanton Waadt): Schweizerische Paläontologische, 87. 1–99.

Robaszynski, F., Caron, M., Amédro, F., Dupuis, C., Hardenbol, J., Gonzalez-Donoso, J.M., Linares, D., Gartner, S., 1994. Le Cénomanien de la région de Kalaat Senan (Tunisie Centrale): litho-biostratigraphie et interprétation séquentielle. Revue de Paléobiologie 12, 351–505.

Robaszynski, F., Hardenbol, J., Caron, M., Amédro, F., Dupuis, C., Gonzalez-Donoso, J.M., Linares, D., Gartner, S., 1993. Sequence stratigraphy in a distal environment: the Cenomanian of the Kalaat Senan region (Central Tunisia). Bulletin du Centre de Recherches et d'Exploration Production Elf-Aquitaine 17, 395–433.

Robaszynski, F., Juignet, P., Gale, A.S., Amédro, F., Hardenbol, J., 1998. Sequence stratigraphy in the Cretaceous of the Anglo-Paris Basin, exemplified by the Cenomanian stage. In: de Graciansky, P.C., Hardenbol, J., Jacquin, T., Vail, P.R. (Eds.), Mesozoic and Cenozoic Sequence Stratigraphy of European Basins. SEPM (Society for Sedimentary Geology), Special Publication 60, pp. 363–386.

Rodriguez-Lazaro, J., Pascual, A., Elorza, J., 1998. Cenomanian events in the deep western Basque Basin: the Leioa section. Cretaceous Research 19, 673–700.

Roth, P.H., 1983. Jurassic and Lower Cretaceous calcareous nannofossils in the western North Atlantic (Site 534): biostratigraphy, preservation, and some observations on biogeography and palaeoceanography. In: Sheridan, R.E., Gradstein, F.M., et al. (Eds.), 1983. Initial Reports of the Deep Sea Drilling Project, 76, pp. 587–621.

Rubino, J.L., 1989. Introductory remarks on upper Aptian to Albian siliclastic/carbonate depositional sequences. In: Ferry, S., Rubino, J.L. (Eds.), Mesozoic Eustacy Record on Western Tethyan Margins. Guide-book of the post-meeting field trip in the Vocontian Trough, 25–28th November 1989. 2ème Congrès Français de Sédimentologie, Lyon, pp. 28–56.

Schlanger, S.O., Jenkyns, H.C., 1976. Cretaceous oceanic anoxic events: causes and consequences. Geologie Mijnbouw 55, 179–184.

Schlanger, S.O., Arthur, M.A., Jenkyns, H.C., Scholle, P.A., 1987. The Cenomanian–Turonian Oceanic Anoxic Event, I. Stratigraphy and distribution of organic carbon-rich beds and the marine $\delta^{13}C$ excursion. Geological Society, London, Special Publication 26, 371–399.

Scholz, G., 1973. Sur l'âge de la faune d'ammonites au Château près de St-Martin-en-Vercors (Drôme) et quelques considérations sur l'évolution des Turrilidés et des Hoplitidés vracono-cénomaniens. Géologie Alpine 49, 119–129.

Scholz, G., 1979. Die Ammoniten des Vracon (Oberalb, Dispar zone) des Bakony-Gebirges (Westungarn) und eine Revision der wichtigsten Vracon-Arten der West-Mediterranean Faunenprovinz. Palaeontographica Abteilung A 165, 1–136.

Stoll, H.M., Schrag, D.P., 2000. High-resolution stable isotope records from the Upper Cretaceous rocks of Italy and Spain: glacial episodes in a greenhouse planet? Geological Society of America, Bulletin 112, 308–319.

Stow, D.A.V., Reading, H.G., Collinson, J.D., 1996. Deep seas. In: Reading, H.G. (Ed.), Sedimentary Environments: Processes, Facies, and Stratigraphy. Blackwell Science, Oxford, pp. 395–453.

Strasser, A., Caron, M., Gjermeni, M., 2001. The Aptian, Albian and Cenomanian of Roter Sattel, Romandes Prealps, Switzerland: a high-resolution record of oceanographic changes. Cretaceous Research 22, 173–199.

Strasser, A., Hilgen, F.J., Heckel, P., 2006. Cyclostratigraphy – concepts, definitions, and applications. Newsletters on Stratigraphy 42, 75–114.

Strasser, A., Hillgärtner, H., Hug, W., Pittet, B., 2000. Third-order depositional sequences reflecting Milankovitch cyclicity. Terra Nova 12, 303–311.

Strasser, A., Pittet, B., Hillgärtner, H., Pasquier, J.-B., 1999. Depositional sequences in shallow carbonate-dominated sedimentary systems: concepts for a high-resolution analysis. Sedimentary Geology 128, 201–221.

Takashima, R., Nishi, R., Hayashi, K., Okada, H., Kawahata, H., Yamanaka, T., Fernando, A.G., Mampuku, M., 2009. Litho-, bio- and chemostratigraphy across the Cenomanian/Turonian boundary (OAE 2) in the Vocontian Basin of southeastern France. Palaeogeography, Palaeoclimatology, Palaeoecology 273, 61–74.

Thierstein, H.R., Roth, P.H., 1991. Stable isotopic and carbonate cyclicity in Lower Cretaceous deep-sea sediments: dominance of diagenetic effects. Marine Geology 97, 1–34.

Thomel, G., 1972. Les Acanthoceratidae cénomaniens des chaînes subalpines méridionales. Mémoire de la Société Géologique de France 116, 1–204.

Thomel, G., 1991. 1- Biostratigraphie et faunes d'ammonites du passage Cénomanien–Turonien dans le Sud-Est de la France. In: Crumière, J.P., Cotillon, P., Schaaf (Coord.), A. (Eds.), Cenomanian–Turonian Boundary Events, Excursion post-colloque dans le Sud-Est de la France. Livret Guide, pp. 57–69.

Thomel, G., 1992. Ammonites du Cénomanien et du Turonien du sud-est de la France, Editions Serre Nice, Tome 1, 422 pp., Tome 2, 384 pp.

Tröger, K.-A., Kennedy, W.J., 1996. The Cenomanian stage. Bulletin de l'Institut Royal des Sciences Naturelles de Belgique (Sciences de la Terre) 66, 57–68.

Uramoto, G.-I., Fujita, T., Takahashi, A., Hirano, H., 2007. Cenomanian (Upper Cretaceous) carbon isotope stratigraphy of terrestrial organic matter for the Yezo Group, Hokkaido, Japan. Island Arc 16, 465–478.

Voigt, S., Gale, A.S., Flögel, S., 2004. Midlatitude shelf seas in the Cenomanian–Turonian greenhouse world: temperature evolution and North Atlantic circulation. Paleoceanography 19, PA4020. http://dx.doi.org/10.1029/2003PA001015.

Wilmsen, M., 2003. Sequence stratigraphy and palaeoceanography of the Cenomanian Stage in northern Germany. Cretaceous Research 24, 525–568.

Wilmsen, M., 2007. Integrated stratigraphy of the upper Lower–lower Middle Cenomanian of northern Germany and southern England. Acta Geologica Polonica 57, 263–279.

Wilmsen, M., Mosavinia, A., 2011. Phenotypic plasticity and taxonomy of Schloenbachia varians (J. Sowerby, 1817) (Cretaceous Ammonoidea). Paläontologische Zeitschrift 85, 169–184.

Wilmsen, M., Niebuhr, B., 2002. Stratigraphic revision of the upper Lower and Middle Cenomanian in the Lower Saxony Basin (northern Germany) with special reference to the Salzgitter area. Cretaceous Research 23, 445–460.

Wilmsen, M., Rabe, M., 2008. Belemnites from the lower middle Cenomanian of Hoppenstedt, northern Germany: significance and integrated correlation. Cretaceous Research 29, 936–942.

Wilmsen, M., Wood, C.J., Niebuhr, B., Zawischa, D., 2007. The fauna and palaeoecology of the Middle Cenomanian *Praeactinocamax primus* Event from the type-locality (Wünstorf quarry, northern Germany). Cretaceous Research 28, 428–460.

Wright, C.W., Kennedy, W.J., 1984. The Ammonoidea of the lower chalk, Part 1. Monograph of the Palaeontographical Society, London 137, 1–126.

Wright, C.W., Kennedy, W.J., 1987. The Ammonoidea of the lower chalk, Part 2. Monograph of the Palaeontographical Society, London 139, 147–218.

Wright, C.W., Kennedy, W.J., 1995. The Ammonoidea of the lower chalk, Part 4. Monograph of the Palaeontographical Society, London 149, 295–319.

Wright, C.W., Kennedy, W.J., 1996. The Ammonoidea of the lower chalk, Part 5. Monograph of the Palaeontographical Society, London 150, 320–403.

Wright, C.W., Wright, E.V., 1949. The Cretaceous ammonite genera *Discohoplites* Spath and *Hyphoplites* Spath. Quarterly Journal of the Geological Society of London 104, 477–498.

Wright, C.W., Calloman, J.H., Howarth, M.K., 1996. Cretaceous Ammonoidea. In: Kaesler, R.L. (Ed.), Treatise on Invertebrate Palaeontology, Part L, Mollusca 4. Geological Society of America, Boulder, CO, and University of Kansas Press, Lawrence, KS, 362 pp.

Appendix

List of ammonoid taxa found in the Blieux section. They are grouped into 11 families, using the supra-specific classification proposed by Wright et al. (1996), emended by the work of Klein et al. (2009).

Involute/evolute planispiral ammonoids:
Acanthoceratoidea Grossouvre
  Acanthoceratidae Grossouvre
    Acanthoceras Neumayr
      A. rhotomagense (Brongniar)
    Cunningtoniceras Collignon
      C. cunningtoni (Sharpe)
      C. inerme (Pervinquière)
    Mantelliceras Hyatt
      M. dixoni Spath
      M. mantelli (Sowerby)
      M. picteti Hyatt
Hoplitoidea Douvillé
  Schloenbachiidae Parona and Bonarelli
    Schloenbachia Neumayr
      S. varians (Sowerby)
  Hoplitidae Douvillé
    Hyphoplites Spath
      H. campichei Spath
      H. costosus Wright and Wright
      H. curvatus (Mantell)
      H. falcatus (Mantell)
Desmoceratoidea Zittel
  Desmoceratidae Zittel
    Puzosia (*Puzosia*) Bayle
      P. (P.) mayoriana (d'Orbigny)
Phylloceratoidea Zittel
  Neophylloceratidae Joly
    Hyporbulites Breistroffer
      H. seresitensis (Pervinquière)
Tetragonitoidea Hyatt
  Tetragonitidae Hyatt
    Tetragonites Kossmat

Heteromorphic ammonoids:
Turrilitoidea Gill
  Turrilitidae Gill
    Hypoturrilites Dubourdieu
      H. mantelli (Sharpe)
      H. tuberculatus (Bosc)
    Mesoturrilites Breistroffer
      M. aumalensis (Coquand)
      M. corrugatus Wright and Kennedy
    Turrilites Lamarck
      T. costatus Lamarck
      T. scheuchzerianus Bosc
  Baculitidae Gill
    Sciponoceras Hyatt
      S. baculoides (Mantell)
  Anisoceratidae Hyatt
    Anisoceras Pictet
      A. plicatile (Sowerby)
  Hamitidae Gill
    Hamites Parkinson
      H. simplex d'Orbigny
  Scaphitoidea Gill
    Scaphitidae Gill
      Scaphites Parkinson
        S. obliquus Sowerby

Appendix A. Supplementary data

Supplementary data related to this article can be found online at http://dx.doi.org/10.1016/j.cretres.2012.06.006.